

# Journal of Soils and Sediments

## Multidisciplinary study of a Holocene sedimentary sequence near Bologna (Italy): insights on natural and anthropogenic impacts on the landscape dynamics

--Manuscript Draft--

<b>Manuscript Number:</b>	
<b>Full Title:</b>	Multidisciplinary study of a Holocene sedimentary sequence near Bologna (Italy): insights on natural and anthropogenic impacts on the landscape dynamics
<b>Article Type:</b>	Research Article
<b>Section/Category:</b>	Soils
<b>Corresponding Author:</b>	Gianluca Bianchini, Prof. University of Ferrara Ferrara, ITALY
<b>Corresponding Author Secondary Information:</b>	
<b>Corresponding Author's Institution:</b>	University of Ferrara
<b>Corresponding Author's Secondary Institution:</b>	
<b>First Author:</b>	Livia Vittori Antisari, Dr
<b>First Author Secondary Information:</b>	
<b>Order of Authors:</b>	Livia Vittori Antisari, Dr Gianluca Bianchini, Prof. Stefano Cremonini, Dr. Dario Di Giuseppe, Dr. Gloria Falsone, Dr. Marco Marchesini, Dr Silvia Marvelli, Dr. Gilmo Vianello, Prof.
<b>Order of Authors Secondary Information:</b>	
<b>Funding Information:</b>	
<b>Abstract:</b>	<p><b>Purpose:</b> This study investigated a Holocene sedimentary sequence evolved from a small catchment located at San Lazzaro di Savena in the surroundings of Bologna Emilia (Northern Italy), in which different buried soil horizons were detected in order to delineate the physiografic evolution of the area.</p> <p><b>Material and methods:</b> Several disciplinary/analytical approaches including pedostratigraphy, geochemistry, radiocarbon dating, archaeobotanical investigation and <sup>13</sup>C/<sup>12</sup>C stable isotopes analyses that were taken into account for the pedosequence characterization.</p> <p><b>Results and discussion:</b> This multidisciplinary approach allowed us to identify the main factors that affected the ancient environment along a prolonged time interval ( 12 ky); starting since 14 ky BP with a paleosoil ascribed to the Bølling period, cold-arid conditions characterized by a steppic vegetation gradually evolved toward a more humid (and slightly warmer) setting. This climatic change allowed the development of a forest constituted by abundant conifers at ca 10 ky BP. Humans also impacted the environment, at least since 9 ky BP, as indicated by repeated traces of firing (plausibly for deforestation and clear land).</p> <p><b>Conclusions:</b> The observed data suggest that human impact on the landscape could have been effective starting from the Mesolithic period, earlier than usually considered by previous studies. These anthropogenic activities favoured geomorphological and hydraulic instabilities, accelerating soil erosion within the basin as indicated by the</p>

	<p>increase of the estimated sedimentation rates and change in the type of geochemical, mineralogical and textural properties of the studied soils. The data allow a comparison with findings provided by other neighbouring sites and contribute to the ongoing debate on the relationships between climatic and anthropogenic impacts on the landscape dynamic.</p>
<b>Suggested Reviewers:</b>	<p>Nicholas Branch , Prof. University of Reading, UK n.p.branch@reading.ac.uk He is an expert of palaeo-environmental reconstructions.</p>
	<p>Stéphanie Desprat , Dr. Université de Bordeaux, France s.desprat@epoc.u-bordeaux1.fr She is an expert of palaeo-environmental reconstructions</p>
	<p>Sebastian Joannin , Dr. CNRS, France sebastien.joannin@univ-montp2.fr He is an expert of palaeo-environmental reconstructions</p>
<b>Opposed Reviewers:</b>	

# Multidisciplinary study of a Holocene sedimentary sequence near Bologna (Italy): insights on natural and anthropogenic impacts on the landscape dynamics

Livia Vittori Antisari <sup>(1)</sup>, Gianluca Bianchini <sup>(\*2)</sup>, Stefano Cremonini <sup>(3)</sup>, Dario Di Giuseppe <sup>(2)</sup>,  
Gloria Falsone <sup>(1)</sup>, Marco Marchesini <sup>(4)</sup>, Silvia Marvelli <sup>(5)</sup>, Gilmo Vianello <sup>(1)</sup>

<sup>(1)</sup> Dipartimento di Scienze Agrarie, Alma Mater Studiorum - Università di Bologna, Via G. Fanin, 40, 40127  
Bologna, Italy

<sup>(2)</sup> Dipartimento di Fisica e Scienze della Terra, Università di Ferrara, Via Saragat 1, 44100 Ferrara, Italy

<sup>(3)</sup> Scienze biologiche, geologiche e ambientali - Alma Mater Studiorum Università of Bologna, Via  
Zamboni 67, 40126 Bologna, Italy

<sup>(4)</sup> Soprintendenza Archeologia dell'Emilia-Romagna, Via delle Belle Arti 52, 40126, Bologna, Italy

<sup>(5)</sup> Laboratorio di Palinologia e Archeobotanica – C.A.A. Giorgio Nicoli – Via Marzocchi 17, 40017 San  
Giovanni in Persiceto, Bologna, Italy

\*Corresponding author: Gianluca Bianchini

## Abstract

*Purpose* This study investigated a Holocene sedimentary sequence evolved from a small catchment located at San Lazzaro di Savena in the surroundings of Bologna Emilia (Northern Italy), in which different buried soil horizons were detected in order to delineate the physiografic evolution of the area.

*Material and methods* Several disciplinary/analytical approaches including pedostratigraphy, geochemistry, radiocarbon dating, archaeobotanical investigation and <sup>13</sup>C/<sup>12</sup>C stable isotopes analyses that were taken into account for the pedosequence characterization.

*Results and discussion* This multidisciplinary approach allowed us to identify the main factors that affected the ancient environment along a prolonged time interval (~ 12 ky); starting since 14 ky BP with a paleosoil

ascribed to the Bølling period, cold-arid conditions characterized by a steppic vegetation gradually evolved toward a more humid (and slightly warmer) setting. This climatic change allowed the development of a forest constituted by abundant conifers at ca 10 ky BP. Humans also impacted the environment, at least since 9 ky BP, as indicated by repeated traces of firing (plausibly for deforestation and clear land).

*Conclusions* The observed data suggest that human impact on the landscape could have been effective starting from the Mesolithic period, earlier than usually considered by previous studies. These anthropogenic activities favoured geomorphological and hydraulic instabilities, accelerating soil erosion within the basin as indicated by the increase of the estimated sedimentation rates and change in the type of geochemical, mineralogical and textural properties of the studied soils. The data allow a comparison with findings provided by other neighbouring sites and contribute to the ongoing debate on the relationships between climatic and anthropogenic impacts on the landscape dynamic.

**Key words:** Holocene sediments; pedology and geochemistry;  $^{14}\text{C}$  dating and palynology;  $\delta^{13}\text{C}$  and carbon speciation, climatic changes;

## 1 Introduction

The interactions between anthropogenic activities and the environment have been correlated throughout the human history. Since the early times, man has modified the environment (e.g. agriculture, grazing, use of fire) (Woodward, 2009 and references within), but in turn anthropogenic activities have been deeply influenced by climatic variability and environmental changes, as demonstrated by paleoenvironmental studies that have shown correlations between climate changes and cultural collapses (Diamond, 2005).

Holocene climate in Europe was punctuated by numerous short-term cold events (Magny et al., 2006; Fleitmann et al., 2007; Yu et al., 2010; Wiersma and Jongma, 2010; Miller et al., 2010; Giraudi et al., 2011; Zanchetta et al., 2012) and these climatic changes were also recorded throughout the Mediterranean region even if their effects varied widely due to local microclimate factors (e.g. Joannin et al., 2013).

According to these climatic variations, during the Middle Holocene, starting from at least 8 ky BP, in many sites of the Northern Apennines the natural vegetation experienced pronounced changes (Branch and Marini, 2013). The initiation and expansion of pastoralism (e.g. leaf foddering) and cultivation further contributed to

1 affect vegetation changes. In several Apennine sites burned biomass were recorded suggesting that burning  
2 was the main deforestation approach for land clearing. The record of these changes was however rarely  
3 preserved in mountain areas, lacustrine basins, and widespread floodplains. Indeed it can be better recorded  
4 in the foothill sedimentary sequences generated by streams having very small catchments. In this study we  
5 investigated a Holocene sedimentary sequence evolved from a small catchment located in Emilia Romagna  
6 (Northern Italy), in which different buried soil horizons were detected. A multidisciplinary approach was  
7 thus carried out in order to assess the relative impact of climatic changes and possible anthropogenic  
8 activities in our study area. Our data give new insights for the scientific debate on the early role of human  
9 forcing on the environment. The topic is extremely important considering that recent findings highlight the  
10 reiterated presence of hominines in the Emilia Romagna Region (Muttoni et al., 2011; Fontana et al., 2013),  
11 followed by documented and recurrent settlements of the Bronze age (Vittori-Antisari et al., 2011; 2013). We  
12 show that detailed multi-proxies investigations (including pedostratigraphy, geochemistry, radiocarbon  
13 dating, pollen and  $^{13}\text{C}/^{12}\text{C}$  stable isotopes analyses) are useful tools for the assessment of the factors that at  
14 local scale affected the ancient environment. Results and assumptions were finally compared with those  
15 obtained from neighbouring sites in order to delineate hypotheses valid at regional scale.  
16  
17  
18  
19  
20  
21  
22  
23  
24  
25  
26  
27  
28  
29  
30  
31

## 32 **2 Geological-geomorphological setting and insights on ancient human settlements**

33  
34 The study site, located in the Municipality of San Lazzaro, 5 km eastward of Bologna, covered an area of  
35 about 2,000 square meters ( $44^{\circ}28'17''$  N,  $11^{\circ}24'34''$  E), at an elevation of 62 m above sea level, in a recently  
36 urbanized area (Figure 1). It is located at the foothill of the Apennine hills and is crossed by the Via Emilia  
37 which is an important route since Roman ages. In particular, the study initiated in connection to a building  
38 excavation that reached the depth of ca 5.5 m, allowing careful field observations and sampling (Figure 1).  
39 From the geomorphological point of view, the building site is located at the outlet of a little hilly catchment  
40 crosscut by a creek known as *Pontebuco stream*. The area consists in a gently sloping alluvial fan (hereon  
41 defined *Pontebuco stream fan*: PSF), 0.9 km<sup>2</sup> wide, hosted between the fan apexes of more important rivers  
42 such as Savena and Zena.  
43  
44  
45  
46  
47  
48  
49  
50  
51  
52  
53  
54  
55

56 Although the manmade modifications performed after the II World War prevent a detailed recognition of  
57 minor landforms, in general the fan topographic surface doesn't show traces of bed entrenchment, suggesting  
58  
59  
60  
61

1 an almost continuous aggradation of the fan structure. Another manmade feature is the prominent break in  
2 slope (ca 20 m/km) characterizing the northern roadway side of the Via Emilia, located less than 100 m south  
3 of the studied stratigraphic site (Fig 1: point 1), due to the diachronic maintenance works performed on the  
4 ancient roman route. Upstream, the Pontebuco stream catchment is composed by the little valleys of two  
5 tributaries flowing mutually parallel. These tributaries are incised 15-30 m in the foothill and 70 m in the  
6 valley head. The whole catchment is on average 3 km long and 0.5-0.6 km large, with local widening related  
7 to ancient slide scars (Fig. 1A). It is reasonable to think that the catchment inception could be dated at around  
8 50-100 ky BP (e.g., Farabegoli et al. 1994), but it is unlikely that the most ancient PSF sedimentary phases  
9 can be recognized due to the sediment mixing with that of the major fans of neighbouring - more important -  
10 rivers Savena and Zena .

11 From the geological point of view, the PSF apex is precisely located at the foothill hinge, where a vertical  
12 tilting is still developing, as result of the mountain chain rising coupled to the alluvial plain subsidence  
13 (Amorosi et al. 1996; Stramondo et al. 2007; Cremonini 2014). This narrow belt corresponds at depth to the  
14 buried Apennine chain main frontal thrust (Martelli et al. 2009; Boccaletti et al. 2011; Picotti et al. 1997;  
15 Picotti and Pazzaglia, 2008).

16 Lithologically, PSF sediments are generally fine grained and the top of the gravel deposits, ascribed to the  
17 Last Glacial Maximum Savena-Zena fluvial system, is lying at ca 9 m below the topographic surface  
18 (Martelli et al. 2009). The understanding of sources of the fan sediments requires some information  
19 concerning the outcropping lithologies. The upper reach of the Pontebuco stream catchment (Fig. 1) is  
20 characterized by the outcrop of Pliocene-Lower Pleistocene marine clays (*Argille Azzurre Formation: FAA*)  
21 (Martelli et al. 2009) in turn overlain by a limited thickness of Lower-Middle Pleistocene littoral sands  
22 (*Sabbie di Imola Formation: IMO*) (Amorosi et al. 1998) outcropping down valley. In the foothill terraces  
23 zone (Fig. 1, point 3) these formations are in turn covered by variously weathered alluvial sediments (*Unità*  
24 *di Bazzano top*) that are 5-7 m thick.

25 The S. Lazzaro foothill physiographic environment is quite rich in archaeological sites spanning from the  
26 Palaeolithic to the protohistory (Nenzioni 1985). No data are known concerning the Roman settlement at S.  
27 Lazzaro, but this silent record can possibly be attributed to burial of the ancient topography.

1 Outcrops preserving ancient traces of human activity have been recorded in the local alluvial sediments  
2 (Cremaschi et al., 1987). Moreover, in the PSF, 200 m northward of the studied stratigraphic site (Fig. 1,  
3 point 2), a 76000 m<sup>2</sup> wide brick-earth quarry (*Fornace Galotti*) excavation removed the natural sediments up  
4 to a depth of more than 5 m allowing to recover archaeological artefacts spanning from the Palaeolithic up to  
5 the Villanovan periods, i.e. the first Iron Age (Nenzioni 1985). During the 20<sup>th</sup> century some scientific  
6 excavations were performed in this quarry recording two peculiar archaeo-stratigraphic settings. The first one  
7 was a small streambed (3 m large, 1 or 2 m deep), SE-NW directed, found at a depth of 2.5 m below ground  
8 level (bgl; Lenzi and Nenzioni 1996, Fig. 1: point 2). Its sandy channel bottom facies contained poorly  
9 reworked elements of Clactonian and proto-Levallois lithic industries, probably eroded by the foothill  
10 terraces. The second archaeo-stratigraphic setting recorded Villanovan age graves (2800-2600 BP) lying  
11 between 2 and 2.7 m of depth, thus referring to a coeval ground surface buried at about 1.5 m of depth  
12 (Scarani 1963). These settings represent two stratigraphic benchmarks useful to constrain the stratigraphic  
13 log of the studied site.  
14  
15  
16  
17  
18  
19  
20  
21  
22  
23  
24  
25  
26  
27  
28  
29

### 30 **3 Materials and methods**

#### 31 3.1 Stratigraphic observations and soil sampling

32 The field observation allowed the distinction of stratigraphic units and buried soil horizons which have been  
33 preliminarily characterized in the field for layer morphology, thickness, particle size distribution, colour and  
34 other textural characters. From the pedological point of view the buried soils were described according to  
35 Schoeneberger et al. (2012) and a sequence of 16 horizons has been recognized and sampled collecting about  
36 1 kg of material from each horizon. A parallel sampling was performed for archaeobotanical (12 samples)  
37 and radiocarbon analyses (3 samples) as detailed below.  
38  
39  
40  
41  
42  
43  
44  
45  
46  
47  
48  
49

#### 50 3.2 Soil analysis

51 The soil samples were air dried and sieved with a 2 mm mesh sieve. The particle size distribution was  
52 determined by the pipette method after dispersion of the sample with a sodium hexametaphosphate solution  
53 (Gee and Brauder, 1986). The pH value was potentiometric determined in a 1:2.5 (w/v) soil:distilled water  
54 suspension with a Crison pH-meter. The electrical conductivity (EC) was also performed in a 1:2.5 (w/v)  
55  
56  
57  
58  
59  
60  
61

soil:distilled water suspension with a Orion conductivity-meter. The carbonate content was measured by volumetric analysis of the carbon dioxide released by a 6 M HCl solution (Loeppert and Suarez, 1996). The total organic C and N has been determined by an elemental CHNS-O EA 1110 Thermo Fisher Scientific; soil samples were weighted in silver pot and treated with HCl to eliminate the inorganic C.

Representative soil samples were selected for mineralogical characterization. The constituent mineralogical phases were identified by X-ray diffraction (XRD) by means of a Philips PW1860/00 diffractometer, using graphite-filtered  $\text{CuK}\alpha$  radiation (1.54 Å). Diffraction patterns were collected in the  $2\theta$  angular range 3–50°, with a 5 s/step (0.02  $2\theta$ ). Soil samples were also analyzed by X-ray fluorescence spectrometry (XRF) as described by Di Giuseppe et al. (2014). The technique enables the identification and quantification of major ( $\text{SiO}_2$ ,  $\text{TiO}_2$ ,  $\text{Al}_2\text{O}_3$ ,  $\text{Fe}_2\text{O}_3$ ,  $\text{MnO}$ ,  $\text{MgO}$ ,  $\text{CaO}$ ,  $\text{Na}_2\text{O}$ ,  $\text{K}_2\text{O}$ ,  $\text{P}_2\text{O}_5$ , expressed in weight percent) and trace (Ba, Ce, Co, Cr, La, Nb, Ni, Pb, Rb, Sr, Th, V, Y, Zn, Zr, Cu, Ga, Nd and Sc expressed in mg kg<sup>-1</sup>) elements. Samples (~ 10 g) were preliminarily quartered and then finely powdered using an agate mortar. Subsequently, an amount of about 4 grams of powder were pressed with addition of boric acid by hydraulic press to obtain powder pellets. Simultaneously, 0.5-0.6 grams of powder were heated for about 12 hours in a furnace at 1000° C in order to determine the LOI value (Loss On Ignition). This parameter measures the concentration of volatile species contained in the sample. The analysis of the powder pellets was carried out using an ARL Advant-XP spectrometer, properly calibrated analyzing certified reference materials. Precision and accuracy calculated by repeated analysis of numerous international standards having matrices comparable with those investigated, i.e. felsic igneous rocks such as granitoids (AC-E, G-2, GA, GH, GS-N, GSR-1, GSP-1) and rhyolites (JR3, RGM1), and various typology of sedimentary rocks (JDO-1, JLK-1, JLS-1, JSD1, JSD2, JSD3), and were generally better than 3% for Si, Ti, Fe, Ca and K, and 7% for Mg, Al, Mn and Na. For trace elements (above 10 mg kg<sup>-1</sup>) errors were generally better than 10%.

Further investigations were obtained using a “Elemental, VARIO MICRO cube” analyzer (combustion mode set at 950 °C) for the analysis of the weight percent of carbon coupled with an Isotopic Ratio Mass Spectrometer (IRMS) Isoprime100 for the analyses of the carbon isotope ratios (<sup>13</sup>C/<sup>12</sup>C). The carbon isotopic composition is given as δ‰ units, with respect to the values of notional standard, which is PDB (Pee Dee Belemnite):  $\delta\text{‰} = (\text{R}_{\text{sample}} - \text{R}_{\text{standard}}) / \text{R}_{\text{standard}} \times 1000$ . The reproducibility and accuracy of spectrometric measurements were controlled by the repeated analyses of laboratory standards. The average δ<sup>13</sup>C standard



deviation was  $\pm 0.1\%$  (Natali and Bianchini, 2015). Analyses were repeated at combustion temperature of 450 °C to measure the carbon content and isotopic signature of the organic matter.

### 3.3 Radiocarbon datings ( $^{14}\text{C}$ )

The radiocarbon datings ( $^{14}\text{C}$ ) were performed by high resolution mass spectrophotometry (AMS) technique. The method described by Calcagnile et al. (2005) and Fiorentino et al. (2008) included a preliminary treatment of the samples following a multi-step protocol that removed sources of contamination and converted material in graphite, the form suitable for AMS analyses. The carbon isotopic ratios were then analysed by comparing the  $^{12}\text{C}$  and  $^{13}\text{C}$  ion beam currents (and in turn the  $^{13}\text{C}/^{12}\text{C}$  ratio expressed as  $\delta^{13}\text{C}$ ) and the  $^{14}\text{C}$  counts for the investigated samples with those obtained for reference materials (e.g.: the fossil wood IAEA C4) of known isotopic composition supplied by the International Atomic Agency (IAEA). The conventional radiocarbon ages were calculated according to Stuiver and Polach (1977), and then converted to calendar ages by using the latest internationally accepted calibration dataset (INTCAL04; Blackwell et al. 2006) and the OxCal 3.1 software (Bronk and Ramsey 2001).

### 3.4 Archaeobotanical analysis

#### 3.4.1 *Pollen analysis*

Palynological analyses were carried out applying a methodology already tested for pollen substrates with some minor modifications (Lowe et al., 1996). The method includes the following phases: about 8-10 g were treated in 10% Na-pyrophosphate to deflocculate the sediment matrix. A *Lycopodium* spores tablet was added to calculate pollen concentration (expressed as pollen grains per gram = p/g). The sediment residue was subsequently washed through 7 micron sieves and then re-suspended in HCl 10% for remove calcareous material and subjected to Erdtman acetolysis; heavy liquid separation method was then introduced using Na-metatungstate hydrate of s.g. 2.0 and centrifugation at 2000 rpm for 20 minutes. Following this procedure, the retained fractions were treated with 40% HF for 24 h and then the sediment residue was washed previously in distilled water and after in ethanol with glycerol; the final residue was desiccated and mounted on slides by glycerol jelly and finally sealed with paraffin. This method preserves the slides for many years after preparation and therefore it is suitable for pollen extractions from geological and archaeological

1 samples. Identification of the samples was performed at 1000 light microscope magnification (ocular 10×  
2 and objective 100×). Determination of the pollen grains was based on the Palinoteca of our Laboratory,  
3 atlases and a vast amount of specific morpho-palynological bibliography. Names of the families, genus and  
4 species of plants conform to the classifications of Italian Flora proposal by Pignatti (1982) and European  
5 Flora (Tutin et al. 1964-1993). The pollen terminology is based on Berglund and Ralska-Jasiewiczowa  
6 (1986), Faegri and Iversen (1989) and Moore et al. (1991) with slight modifications that tend to simplify  
7 nomenclature of plants. The term “taxa” is used in a broad sense to indicate both the systematic categories  
8 and the pollen morphological types (Beug 2004). Identified pollens (between 300 and 400 grains) have been  
9 expressed as percentages of the total.  
10  
11  
12  
13  
14  
15  
16  
17  
18  
19  
20

#### 21 3.4.2 *Microanthracological analysis*

22  
23 The same samples prepared for pollen analysis were also investigated for the identification of  
24 microcharcoals. Microanthracological analysis has been used to understand past fire events mostly connected  
25 to anthropogenic activities. Point count estimation of microscopic charcoal abundance was carried out, and  
26 charcoal fragments encountered during pollen counting were recorded in four size classes, based on long axis  
27 length (10-50 µm, 50–125 µm, 125-250µm, >250µm) (Whitlock and Millspaugh, 1996; Clark 1982; 1997;  
28 Patterson et al. 1987; Whitlock and Larsen 2001). The former two classes are thought to be wind-blown  
29 transported hence giving informations concerning the regional fire events, whereas the latter two are  
30 considered the result of local vegetation burning.  
31  
32  
33  
34  
35  
36  
37  
38  
39  
40  
41  
42

#### 43 3.4.3 Anthracological analysis

44  
45 During the excavation 26 carbonized trunks (from 30 to 50 years old) were found at 3.84 m depth (Fig. 2); in  
46 the field were collected subsamples with a size of about 2.5-5.0 cm<sup>3</sup> for the identification. In laboratory they  
47 were identified using a reflected light microscope with the help to the anthraco-xylological reference  
48 collection and on the keys and atlases (Grosser 1977, Hather 2000, Jacquot et al. 1973, Schweingruber  
49 1990).  
50  
51  
52  
53  
54  
55  
56  
57  
58

#### 59 3.5 Statistical analysis

1 A multivariate statistical approach has been useful to investigate the multi-elementary chemical data  
2 provided by XRF of the considered horizons highlighting chemical analogies and differences between the  
3 samples, and delineating different sample groups. In this study, we used a combination of Principal  
4 Component Analysis (PCA) to correlate the measured parameters. A comprehensive mathematical/statistical  
5 description of the method is provided by Jolliffe et al. (2002). Through PCA, the observed elemental  
6 correlations were grouped in a small number of factors that account for most of the variance of the  
7 considered dataset. In particular, this elaboration was carried out by the SPSS (Release 17.0, Lead  
8 Technologies, demo version), using Varimax with Kaiser Normalization as rotation method, as suggested by  
9 Facchinelli et al. (2001). On the basis of eigenvalues greater than one, four factors were selected for  
10 explaining 86.9% of the cumulative total variance.  
11  
12  
13  
14  
15  
16  
17  
18  
19  
20  
21  
22

## 23 **4 Results**

24  
25 The Figure 2 synthesizes the multidisciplinary results obtained in this study. More detailed information  
26 concerning the various type of results were reported in the distinct paragraphs reported below. Although no  
27 significant archaeological items were found, the archaeological survey suggested the possible existence of  
28 three topographic surfaces characterized by human frequentation, buried at 1.85, 3.47 and 4.75 m of depth,  
29 respectively (Figure 2). The former level recorded some sherds probably dating to the Iron Age. The latter  
30 two levels did not record any trace of archaeological materials, but are characterized by postholes-like traces.  
31  
32  
33  
34  
35  
36  
37  
38  
39  
40

### 41 **4.1 Stratigraphy and soil sequences**

42  
43 Down to a depth of 5.5 m below ground level the stratigraphic study highlighted four main distinct  
44 sedimentary sets, probably representing different sedimentary phases, where distinct soils have been  
45 recognized and described in Table 1 according to Schoeneberger et al. (2012)  
46  
47  
48  
49

50 From a stratigraphic viewpoint the site showed a horizontal, tabular layering very slightly dipping eastwards.  
51 The first set was recognizable down to the depth of 1.85 m, while the other three were separated by marked  
52 discontinuities at the depths of 3.65 m, 4.45 m, 5.25 m, respectively.  
53  
54  
55

56 The uppermost set (including S1-S5 soil samples) consisted in a fining upward sequence with the sandy  
57 basal layer (35 cm thick) laterally continuous for tens of metres, possibly related to a splay deposit from an  
58  
59  
60  
61

unconfined water current, thus resembling an alluvial fan lobe rather than a lateral crevasse splay. The sand layer contains granules and very small cherty pebbles suggesting that the clastic particles come from the *Sabbie di Imola* formation (IMO; Figure 1B). Some rounded fragments of Roman Age bricks were also found in the sand basal layer. The profile of this set was formed by the following horizons: Apb/ABcb/Bwcb/C1/C2 (from S1 to S5 soil samples; Fig. 2). The Bw horizon was recognized by both root sheaths and prismatic soil structures (Table 1), whereas C1 (S4) was a horizon with a natural high amount (50%) of rounded rock fragment and a coarse (sand) texture. Below the lower limit (C2 soil horizons) of this set a sharp lithological discontinuity was observed.

The second set (samples S6-S10), down 3.65 m, had a quite homogenous silty-clay texture (Table 1) and was characterized by a 2Bcb/2Bcssb1/2Bcssb2/2Bckb1/2Bckb2 sequence of horizons. Almost all the horizons were characterized by many mottles, a blocky angular structure, with sticky consistence, carbonate nodules/concretions and without skeleton. Hard breaking strength distinguished the dried samples, that were also characterized by presence of slickenside (S7 and S8 layers) having at least 4 cm<sup>2</sup> extension; the S9 and S10 soil samples (corresponding to 2Bckb1 and 2Bckb2 horizons) were characterized by pedogenetic carbonate nodules. At the boundary between S9 and S10, at the depth of 3.35 m, a bone fragment was found, while a charcoal useful for <sup>14</sup>C dating was sampled between 2Bcb and 2Bcssb1 (S6 and S7 soil samples, respectively; Figure 2).

The third set (down to 4.45 m of depth) consisted of variously darkened layers (S12 and S13) and its upper limit was marked by the lithological discontinuity in the 3Bcb horizon (S11 soil sample). The 3Bcb horizon was characterized by the presence of carbonate masses of primary origin (i.e. residues of the parent material). The S12 and S13 layers were coded as 4Ab1 and 4Ab2 due to the textural change with marked increase in the clay content (silty-clay texture; Table 2) with respect the overlying horizon, highlighting the presence of another lithological discontinuity; furthermore, some features like a dark colour (10YR5/3 and 10YR4/2, respectively), hard consistence and plastic character and also carbonate masses and concretions were observed. A burnt tree was sampled between these two horizons.

The fourth set (down to the bottom of the excavation, including S14-S15 samples) was characterized by a change of texture (clay-loam) identifying a further lithological discontinuity. Granular structure, dark colour (10YR3/3) and mottles (10YR5/6) characterized the S14 horizon, whereas S15 showed reddish colour

(2.5Y6/6) with mottles (10YR6/8) and a subangular blocky structure. These features suggested 5Ab and 5Bwcb horizons sequence, respectively. In the deepest S16 horizon, an additional discontinuity marked by a further change in the texture (loam) was detected. Yellowish brown colour, with presence of mottles (10YR6/8) and carbonate nodules allowed to code this horizon as 6Bwcb (Figure 2 and Table 2).

#### 4.2 Physico-chemical soil properties

The Table 2 shows the main physicochemical soil properties. The pH values ranged from 7.6 to 8.2; generally the total carbonate content was low (from 9 to 60 g kg<sup>-1</sup>), increasing only in the horizons marking sharp lithological discontinuities (103 and 153 g kg<sup>-1</sup> for S11 and S16, respectively). The organic C content ranged from 1.4 to 8.3 g kg<sup>-1</sup>; the C1 and C2 layers had the lowest organic C amount <2 g kg<sup>-1</sup>, whereas the highest organic C content was detected in the lowest Ab horizons (S12, S13, and S14 samples coded as 4Ab1, 4Ab2 and 5Ab horizons, respectively).

The box plots of Figure 3, obtained for the different sets of samples recognized along the stratigraphy, show an increase of pH values in the second and third sets, associated to a slight increase of carbonate. An increase of organic C and total N along the depth of sequence is also noticed. The sand and clay contents confirmed the existence of lithological discontinuities already observed during the field survey.

The mineralogical composition of the first three sets has been investigated by X-ray diffractometry (XRD). In the most superficial set (sample S2) the dominant mineral phase was quartz, with only minor sporadic amount of calcite and phyllosilicates, whereas in the second (sample S8) and third (sample S12) sets the amount of quartz decreased, while calcite and phyllosilicates progressively increased (Figure 4).

The geochemical composition expressed by the amount of major and trace elements (Table 3) reflected the differences in the mineralogical composition observed in the distinct sets. Elaboration of these data by Principal Component analysis (PCA) allowed to identify the geochemical analogies and differences between soil samples of the distinct sets. In fact, the defined sets broadly corresponded to homogeneous families having distinctive geochemical features (Figure 5), suggesting that the pedological sequence ranging from S1 to S5 had a homogeneous geochemical affinity. A second homogeneous family extended from the layers S6 to S10. The deeper part of the excavation was less homogeneous and from the geochemical point of view differences between S12 -S13 and S14-15 horizons were observed.

1 High content of quartz fitted with the very high SiO<sub>2</sub> content (65-78 wt%) of the first set, and comparatively  
2 low Al<sub>2</sub>O<sub>3</sub> (<15.8 wt%) and CaO (<0.95 wt%) percentage confirmed the low amount of phyllosilicates (such  
3 as clay minerals) and very low carbonate content. The second set, from S6 to S10 samples, was totally  
4 different from the more superficial first set due to the lower SiO<sub>2</sub> content (55.3-61.1 wt%) and higher Al<sub>2</sub>O<sub>3</sub>  
5 and CaO amount (15.8-17.8 and 1.0-6.1 wt%, respectively), thus confirming the greater content of  
6 phyllosilicates and calcite that was recorded by XRD. The soil samples of this set were also enriched in many  
7 trace elements such as Ni, V, Sc, Rb, Ba, La, Nd, Th, Nb (Table 3; Figure 6) that can be hosted by  
8 phyllosilicates such as smectite, chlorite and other accessory femic minerals. Within the second set, SiO<sub>2</sub>  
9 percentage decreased systematically from the most superficial horizon (2Bcb) to the deepest one (2Bckb2),  
10 whereas on the contrary CaO (and Sr) content increased.

11 The difference in SiO<sub>2</sub>, Al<sub>2</sub>O<sub>3</sub>, CaO between S12-S13 (55.4-58.2 wt%, 17.7-17.8 wt%, 1.6-3.0 wt% for S12  
12 and S13, respectively) and S14-S15 samples (61.9-62.8 wt%, 16.4-16.9 wt%, 1.3-1.5 wt%, for S14 and S15,  
13 respectively) suggested that these horizons belonged to distinct sedimentary phases. The trace element  
14 distribution (Figure 6) seemed to further support this hypothesis.

15 The deepest investigated sample (S16) seemed a further independent soil, which reflected a significant  
16 presence of geogenic carbonates testified by very high Ca and Sr content.

17 The elemental-isotopic results of both total C (C<sub>tot</sub>) and organic C (C<sub>o</sub>) carried out on the studied  
18 pedostratigraphic sequence are reported in Table 4 and Figure 7. C<sub>o</sub> should complement the inorganic carbon  
19 fraction C<sub>i</sub> (that can be inferable by the CaCO<sub>3</sub> content of Table 2) and the sum of two fractions (C<sub>o</sub>+C<sub>i</sub>)  
20 should be conformed to the measured C<sub>tot</sub> as following: C<sub>o</sub>+C<sub>i</sub>=C<sub>tot</sub>.

21 It can be observed that the C<sub>tot</sub> content varied between 0.9 and 2 wt%, while the related δ<sup>13</sup>C ranged between  
22 -11.4 and -24.7 ‰ (Table 4). These C<sub>tot</sub> isotopic values were the result of mixing between organic matter  
23 (usually characterized by strongly negative isotopic values) and carbonates which were characterized by  
24 δ<sup>13</sup>C~ 0 ‰. Coherently, the less negative isotopic values marked perfectly the carbonate-rich horizons. The  
25 carbon isotopic composition of the organic fraction had a much more homogeneous δ<sup>13</sup>C between -23.6 and -  
26 25.2 ‰.

27 A misfit between the measured C<sub>tot</sub> and the calculated one (C<sub>o</sub>+C<sub>i</sub>) was also investigated, and this deficiency  
28 (ΔC) was recorded in the most superficial S1 horizon and in the horizons S12, S13, S14. This parameter

1 highlighted the presence of a further carbon fraction that was not recorded, plausibly represented by black  
2 (elementary) charred carbon. The elementary carbon detected in the deep S12, S13, S14 was probably related  
3 to fires and biomass burning (i.e. burnt trees).  
4  
5  
6

#### 7 4.3 <sup>14</sup>C Datings 8

9 The studied stratigraphic sequence contained very few materials suitable for radiocarbon dating: the  
10 uppermost sample was represented by charred carbon fragments of the sample S6 (Figure 2); an intermediate  
11 sample was a large fragment of mammal bone that was lying between S9 and S10, while the deepest material  
12 was represented by combustion residua of tree trunks collected in correspondence of the S12 (Figure 2).  
13  
14  
15  
16  
17

18 The obtained 1σ confidence level, calibrated <sup>14</sup>C datings provided ages of 6660-6530 y BP, 8330-8190 y BP,  
19 and 9270-9090 y BP.  
20  
21  
22

23 At a first instance, these values are positively correlate with a downward trend whose end-member was the  
24 deepest paleosol which should have an age of ca 14-15 ky BP (see below). However, the most recent  
25 radiocarbon age (6660-6530 y BP) in horizon S6 is diachronic with the finding of Villanovan artefacts which  
26 should correspond to ca 2800-2600 y BP. The temporal gap between the radiometric age and the  
27 archaeological constraint has to be taken into account and will be discussed in the next section.  
28  
29  
30  
31  
32  
33  
34  
35

#### 36 4.4 Archaeobotanical analysis 37

##### 38 4.4.1 *Pollen analysis* 39

40 Pollen grains were found in all samples in a good state of preservation, allowing the identification of most of  
41 the cases. In total 3850 pollen grains were counted. Pollen concentrations were variable depending on the  
42 richness of organic matter and the preservation conditions. They ranged from 10<sup>2</sup> to 10<sup>3</sup> p/g most samples,  
43 and only the samples S15, S14 and S4 were comparatively poor of pollen grains (less than 10<sup>2</sup> p/g).  
44  
45  
46  
47  
48

49 The pollen flora, consisted of 92 types (31 trees, shrubs, lianes and 61 herbs) and is synthetized in Figure 2.

50 The sample S16 was characterized by high presence of *Compositae* family (81.2%) especially *Cichorioideae*  
51 and *Asteroideae*, followed by *Gramineae* spontaneous group (6.7%) with only low percentages of *Pinaceae*  
52 (1.8%). *Dryas octopetala* pollen grains were also detected (1.2%). This pollen grains association indicates a  
53 landscape developed on steppic conditions (dry and cold) typical of late glacial period.  
54  
55  
56  
57  
58  
59  
60  
61

1 The samples S15 and S14 revealed a high percentage of *Pinus*, followed by *Cichorioideae* and *Gramineae*  
2 spontaneous group which indicates a transition between the steppic condition delineated above and a  
3 landscape dominated by conifers, possibly occurred in the Preboreal period.  
4

5 The sample S13 (the lowest horizon of the third stratigraphic set), containing more pollen grains (and more  
6 pollen species), showed a drastic decrease of *Cichorioideae*, a more diversified association of *Pinus* species  
7 coupled with the appearance of *Quercus* deciduous (especially *Quercus* cf. *robur*), *Ostrya carpinifolia*/*C.*  
8 *orientalis*, *Fraxinus excelsior*, *Tilia*, *Ulmus* and *Corylus*. This rich biodiversity suggests an important  
9 climatic change with the establishment of more temperate conditions. Noteworthy, this horizon corresponds  
10 to the surface where the burnt oak trees were rooted and it can be assigned to the Preboreal (ca. 11.7-10 ky  
11 BP).  
12  
13  
14  
15  
16  
17  
18  
19

20 The samples S12, S9 and S8 were characterized by a further increase of coniferous pollens; in particular S12  
21 corresponded to the part of the sequence where the burned wooden logs (9270-9090 cal y BP) were found.  
22 These horizons were characterized by the significant presence of linden and white fir, which plausibly  
23 ascribe them to the Atlantic period (Accorsi et al. 1996, 2004 ).  
24  
25  
26  
27  
28  
29

30 In the sample S9 and S8 the decrease of *Pinaceae* taxa was connected with an increase of *Corylus*, *Ulmus*  
31 and *Tilia*, which could suggest a weak opening in the vegetation cover. This process was accompanied by the  
32 presence or expansion of taxa indicative of human impact (e.g. *Cerealia*).  
33  
34  
35

36 In the sample S6 an increase of *Compositae* (45.8%) coupled with *Plantaginaceae*, *Ranunculaceae* and  
37 *Sparganiaceae*/*Typhaceae* and also *Gramineae* spontaneous group and *Leguminosae* (about 4.2% for each  
38 species) has been observed.  
39  
40  
41  
42

43 The vegetation suffered a further sharp change in correspondence of sample S2 (first stratigraphic set) where  
44 it can be observed an additional anthropogenic influence demonstrated by high *Cerealia* diffusion with the  
45 presence of pollen grains of both *Hordeum* and *Avena-Triticum* groups, together with pollen grains ascribed  
46 to *Triticum* cf, *spelta* and *Secale cereal*. Further proxies of human activities were represented by  
47 *Chenopodiaceae*, *Plantago*, *Rumex*, *Urtica dioica*, etc.  
48  
49  
50  
51  
52  
53  
54  
55  
56

#### 57 4.4.2 Microanthracological analysis 58 59 60 61 62 63 64 65



1 Among the 12 studied samples, the total micro-charcoal concentration of 10 samples was lower than 0.5  
2 mm<sup>2</sup>/g; this concentration plausibly represents representing the local background. Samples S13 and S12  
3 contain a decidedly higher micro-charcoal concentration (8.9 and 4.9 mm<sup>2</sup>/g, respectively). Micro-charcoal  
4 grains in S13 were characterized by 10-125 µm and is ascribed to a regional fire event, whereas micro-  
5 charcoal grains in S12 contain both the 10-125 and >125 µm size classes possibly indicating a local fire  
6 event. Therefore the local, direct burning effect is highlighted by sample S12, whereas the evidence of  
7 sample S13 could be assigned to an to independent (older) burning effects from a neighbouring area and/or  
8 to post-depositional processes reworking the grains of the overlying horizons.  
9  
10  
11  
12  
13  
14  
15  
16  
17  
18

#### 19 4.4.3 *Anthracological analysis*

20  
21 The charcoal analysed comes from 26 burnt trunks; generally the charcoal was found in a better state of  
22 preservation. The anthracological flora include 2 taxa: *Quercus* cf. *robur* (16 anthracological records) and  
23 *Quercus* undiff. (6 anthracological records); 4 anthracological remains are not undeterminable. All of them  
24 are regional deciduous oaks.  
25  
26  
27  
28  
29  
30  
31  
32  
33

## 34 5 Discussion

35  
36 The studied stratigraphic suite developed in an alluvial environment along the PSF longitudinal axis  
37 generated by a few kilometres scale catchment. The sedimentary record began since the last Late Glacial  
38 period, as indicated by the integration of pollen, radiocarbon and soil data. In particular, the pollen analysis  
39 can provide clues on the past climatic conditions and chronological thresholds (Orombelli and Ravazzi  
40 1996).  
41  
42  
43  
44  
45  
46

47 The sedimentation rates in the studied site were calculated using the sediment thickness and the  
48 chronological data (Fig. 2; Table 1). In these calculations, we considered the radiocarbon ages, the  
49 conventional ages of 14.5 ky BP for the Bølling paleosoil, 3 ky BP for the Iron Age, and 2 ky BP for the top  
50 of the natural sequence. The sedimentation rates (mm/y) resulted to be 0.2 during Late-Glacial and Preboreal  
51 (samples S15 to S12), 1.2 during Boreal/Atlantic (Mesolithic: samples S12 to S9), 0.8 during the Atlantic  
52 (samples S9 to S6), 1.4 during the Late-Antiquity (samples S5 to S1). Although aware that estimations can  
53  
54  
55  
56  
57  
58  
59  
60  
61

1 be influenced by the Sadler effect, implying lowering of the sedimentation rates for investigation of  
2 longer/older time spans (Bianchini et al. 2014), we suggest that in the studied sequence a significantly  
3 increase of the sedimentation rate occurred since the Mesolithic. The high sedimentation rate recorded during  
4 the Boreal/Atlantic period was plausibly due to higher erosion rate within the Pontebuco stream catchment,  
5 preferentially affecting the outcropping area of the *Argille Azzurre* Formation (marly-clays). The more  
6 marked sediment supply to the Pontebuco stream, in turn favoured a more effective aggradation of  
7 Pontebuco stream fan (PSF). These conditions were probably triggered by more marked precipitations.  
8  
9

10 The basal sample S16 sample characterized by significant amount of geogenic carbonate (high percentage of  
11 Ca and Sr) and by the presence of pioneer herbaceous taxa usually considered "aridity markers" (i.e.  
12 *Artemisia*) coupled with *Dryas octopetala*, suggest a cold and arid environment. In our view, S16 can be  
13 attributed at least to the Older Dryas period (ca. 15 ky BP) for its stratigraphic location below the horizon  
14 S15 which is characterized by typical Bølling soil features. This steppic vegetation is recorded in numerous  
15 regional pollen records of the same time period (Watts et al. 1996; Magri and Sadori 1999; Ammann et al.  
16 2000; Deneffe et al. 2000; von Grafenstein et al. 2000; Allen et al. 2002; Bordon et al. 2009; Kotthoff et al.  
17 2008; Combourieu-Nebout et al. 2009; Fletcher et al. 2010; Desprat et al. 2013) indicating that cold-arid  
18 climate conditions were prevailing over the whole Mediterranean basin and especially in the  
19 Padanian/Adriatic basin.  
20  
21

22 In fact, the overlying soil S15 can be considered a benchmark soil assigned to the final part of the the Bølling  
23 period (ca. 15-14 ky BP) related to more wet and warm climate conditions (Frisia et al. 2005; Baroni et al.  
24 2006). It is well known that similar climatic conditions have led to the development of Xeralf (Soil Survey  
25 Staff 2014) named in Emilia-Romagna Region as *Vignola Unit soil* (Gasperi et al. 1989). These paleosoils  
26 were found along the Apennine chain foothill (Cremonini et al. 2012) as well as in the pedeaipine plain  
27 (Cremaschi 1987; Ravazzi et al. 2012; Cremaschi and Nicosia, 2012). The increase of *Pinus* indicates a  
28 vegetation transition between steppic environment toward a landscape dominated by conifers, that can be  
29 associated to the formation of Alfisols under natural wood cover and xeric pedoclimate conditions  
30 (Cremaschi and Nicosia 2012).  
31  
32

33 The dark (S14) and reddish (S15) horizons formed a pedosequence composed by 5Ab and 5Bwcb  
34 characterized by few pollen grains. The scarce presence of pollens should indicate a climatic transition  
35  
36

1 occurred in the Younger Dryas/Preboreal period. In spite of a relative paucity of pollens, the very dark S14  
2 sample had high content of elemental C that was detected by a misfit between  $C_{tot}$  and that calculated by  
3  $(C_o+C_i)$ . This deficiency ( $\Delta C$ ) can be allocated to black (elemental) charred carbon related to fires and  
4 biomass burning. Similar dark soils were found in other sites of the Emilia-Romagna Region (e.g. Alessio et  
5 al. 1980; Ravazzi et al. 2006; Cremonini et al 2007), also in distal plain facies such as probably the *Argille di*  
6 *Vedrana*, and although they are not all strictly coeval they could be interpreted as pedomarkers developed  
7 between Younger Dryas and Boreal chronozones (Ammann et al., 2000; von Grafenstein et al. 2000). In the  
8 city of Bologna a pollen sterile black-soil of similar thickness was dated by radiocarbon at 9300-8650 BP  
9 (Cremonini et al. 2007; Cremonini et al 2012; Amorosi et al. 2014).

10 The S13 sample (4Ab2 horizon) in the third stratigraphic set corresponds to the surface where the burnt oak  
11 trees were rooted and can be assigned to the Preboreal/Boreal period, as also suggested by the burned oak  
12 trunk of S12 horizon dating ~ 9.1 ky BP. The pollens in the S12 sample suggest that vegetal cover  
13 progressively developed during the Holocene (Accorsi et al. 1999) in the Boreal to Atlantic time interval.  
14 This horizon also records evidence of charred material, given by the occurrence of relics of combusted oak  
15 trees, as also confirmed by the  $\Delta C$  parameter indicating the presence of elemental carbon. This suggests the  
16 occurrence of fires and biomass burning, possibly resulting from man-made deforestation practices, as  
17 suggested for other sites of northern Italy (Vescovi et al. 2010).

18 The above lithological discontinuity (S11 sample), that marked the upper limit of the third set, suggests a  
19 sharp variation toward warmer conditions attested by the decline of *Picea* and *Abies* and the increase of  
20 *Tiliaceae*.

21 This climatic change is coupled with the above mentioned anthropogenic influence testified by several  
22 evidence of biomass burning. These findings are in agreement with several anthropogenic indicators of  
23 Neolithic settlement (ca. 7950 y BP) in many Italian sites (Bellini et al. 2009; Rottoli and Castiglioni 2009;  
24 Joannin et al. 2013).

25 Noteworthy, in other North Apennines sites, during the mid-Holocene ca. 6450 y BP and ca. 2950 y BP *Abies*  
26 declined, even if these vegetation changes in distinct sites were probably not synchronous due to  
27 superimposition of local micro-climatic effects on more general climatic changes, and/or to local  
28 geological/pedological factors, as well as to human impacts (Vescovi et al. 2010). Similar evidences were

1 recorded at ca. 6650 and ca. 5950 y BP in the stratigraphy of the study-site site Lake Ledro (Joannin et al.  
2 2013).

3 In the investigated site of S. Lazzaro relatively homogeneous environmental conditions persisted for a long  
4 period until the formation of sample S6, which in spite of the radiometric age of ~ 6550 y BP also  
5 represented a topographic surface of the first Iron Age (Villanovan). In other words, the existence of charcoal  
6 dating to ~ 6550 y BP in this layer implies that this surface could have been exposed to the atmosphere for  
7 ~ 3500 years between the Neolithic and the Iron Age. In spite of the long soil development, the complete soil  
8 profile is missing and ~ 30 cm of surficial horizons (A) are totally lacking, thus marking a significant  
9 erosional process.

10 This framework is coherent with the paleogeographic reconstruction provided by palynology, which  
11 indicates a change of pristine forest condition with appearance of plants introduced by human activities. The  
12 stable isotopic values of organic C are similar to those recorded by Vittori Antisari et al. (2013) in a  
13 neighbouring excavation (down to a depth of 4.5 m) which recorded soil samples having  $\delta^{13}\text{C}$  between -23.8  
14 and -26.6 ‰ (Figure 7). These isotopic values on the soil organic fraction are obviously related to the type of  
15 existing vegetation, and according to Meier et al. (2014) a similar  $\delta^{13}\text{C}$  range reflects a clear predominance  
16 (~80%) of plants having C3 photosynthetic pathway.

17 A further abrupt change is testified by the different features recorded in the most superficial horizons  
18 between the S5 and S1 samples forming the first set. The textural, mineralogical and geochemical data of  
19 these layers indicate that the source of detritus was displaced toward an area dominated by the *Sabbie di*  
20 *Imola* Formation (IMO, quartz-rich sands) and older soils resembling those currently recognized in the  
21 terraces of the basin (AES<sub>6</sub>, Figure 1B). The related soil profile appears to be very poorly developed,  
22 probably indicating continuous sedimentation pulses arriving through the time. During this later period,  
23 *Pontebuco stream* possibly experienced high energy, episodic sheet-floods as demonstrated by the S4  
24 sample containing un-classed pebbles and gravel. Subsequently, the PSF area suddenly become quiescent  
25 and terminated its aggradation, probably due to human intervention aimed to minimize the flood risks for the  
26 human settlement. This happened during Roman times.

## 27 **6 Conclusion**

1 The presented data emphasize the importance of alluvial sediment and soil investigations to elucidate  
2 fluctuations of environmental conditions, including climatic changes and past anthropogenic impacts on the  
3 natural landscape. In particular, the considered stratigraphic sequence exposed in the locality of San Lazzaro  
4 di Savena (Bologna, Italy) provides information on the Holocene evolution of the northern foot-hill  
5 Apennine area, suggesting that at the beginning of this period the climate was quite cold and relatively arid  
6 favouring a steppic vegetation growth. With the Holocene inception a slight increase in the temperature and  
7 an increase of precipitations favoured the development of forest constituted by abundant conifers. Humans  
8 impacted this environment making fires during the Mesolithic to clear the area and during the Neolithic to  
9 obtain soils for agriculture and animal farming. The human presence favoured geomorphological and  
10 hydraulic instabilities, accelerating soil erosion. Therefore the observed data suggest that human impact on  
11 the landscape started to be effective in the Mesolithic period, earlier than usually considered by previous  
12 studies. Finally, more recent (probably Roman age) hydraulic works confined the *Pontebuco stream* leading  
13 to the inactivation of his alluvial fan area, rendering the surrounding lands stable for settlements.  
14  
15  
16  
17  
18  
19  
20  
21  
22  
23  
24  
25  
26  
27  
28  
29

### 30 **Acknowledgement**

31 A special thank must be addressed to Giuliana Steffè and Valentina Manzelli (Soprintendenza Archeologia  
32 dell'Emilia-Romagna) and to C. Mazzoni (Soc. Coop. Archeologia) for the helpful discussion and  
33 information. The authors are also grateful to R. Tassinari that carried out the XRF analyses at the University  
34 of Ferrara.  
35  
36  
37  
38  
39  
40  
41  
42

### 43 **References**

- 44  
45 Accorsi CA, Bandini Mazzanti M, Mercuri AM, Rivalenti C, Trevisan Grandi G (1996) Holocene forest pollen  
46 vegetation of the Po plain - Northern Italy (Emilia Romagna data). *Allionia* 34: 233-276  
47  
48  
49  
50  
51 Accorsi CA, Bandini Mazzanti M, Forlani L, Mercuri AM, Trevisan Grandi G (1999) An overview of Holocene forest  
52 pollen flora/vegetation of the Emilia Romagna region - Northern Italy. *Archivio Geobotanico* 5: 3-27  
53  
54  
55  
56  
57 Accorsi CA, Bandini Mazzanti M, Forlani L, Mercuri AM, Trevisan Grandi G (2004) Holocene forest vegetation  
58 (pollen) of the Emilia Romagna Plain - Northern Italy. *Colloques Phytosociologiques* 28: 1-103  
59  
60  
61  
62  
63  
64  
65

- 1 Alessio M, Allegri L, Bella E, Calderoni G, Cortesi G, Cremaschi M, Improta S, Papani G, Petrone V (1980) Le  
2 datazioni <sup>14</sup>C della pianura tardo-wurmiana ed olocenica nell'Emilia occidentale. Contributi preliminari alla  
3 realizzazione della Carta Neotettonica d'Italia (P.F. Geodinamica), Pubbl n 356: 1411-1435  
4  
5  
6  
7  
8 Allen JRM, Watts WA, McGee E, Huntley B (2002) Holocene environmental variability - the record from Lago Grande  
9 di Monticchio, Italy. Quatern Int: 88: 69-80  
10  
11  
12  
13  
14 Ammann B, Birks HJB, Brooks SJ, Eicher U, Grafenstein von U, Hofmann W, Lemdahl G, Schwander J, Tobolski K,  
15 Wick L (2000). Quantification of biotic responses to rapid climatic changes around the Younger Dryas - a  
16 synthesis. Palaeogeogr Palaeoclimatol Palaeoecol 159: 313-347  
17  
18  
19  
20  
21  
22  
23 Amorosi A, Farina M, Severi P, Preti D, Caporale L, Di Dio G (1996) Genetically related alluvial deposits across active  
24 fault zones: an example of alluvial fan-terrace correlation from the upper Quaternary of the southern Po Basin,  
25 Italy. Sediment Geol 102: 275-295  
26  
27  
28  
29  
30  
31 Amorosi A, Caporale L, Cibir U, Colalongo ML, Pasini G, Ricci Lucchi F, Severi P, Vaiani SC (1998) The Pleistocene  
32 littoral deposits (*Imola Sands*) of the Northern Apennines piedmont. Giornale di Geologia 60: 83-118  
33  
34  
35  
36  
37 Amorosi A, Bruno L, Rossi V, Severi P, Hajdas I (2014) Paleosol architecture of a late Quaternary basin-margin  
38 sequence and its implications for high-resolution, non-marine sequence stratigraphy. Global Planet Change 112:  
39 12-25  
40  
41  
42  
43  
44  
45 Baroni C, Zanchetta G, Fallick AE, Longinelli A (2006) Mollusca stable isotope record of a core from Lake Frassino,  
46 northern Italy: hydrological and climatic changes during the last 14 ka. The Holocene 16: 827-837  
47  
48  
49  
50  
51 Bellini C, Mariotti-Lippi M, Montanari C (2009) The Holocene landscape history of the NW Italian coasts. The  
52 Holocene 19: 1161-1172  
53  
54  
55  
56  
57 Berglund BE, Ralska-Jasiewiczowa M (1986) Pollen analysis and pollen diagrams. In Berglund BE (Ed) Handbook of  
58 Holocene Palaeoecology and Palaeohydrology, Wiley, Chichester pp 455-484.  
59  
60  
61  
62  
63  
64  
65

- 1 Beug HJ (2004) Leifaden der Pollenbestimmungen für Mitteleuropa und angrenzende Gebiete. Verlag Friedrich Pfeil,  
2 Munich, pp 54.  
3  
4  
5  
6 Bianchini G, Cremonini S, Di Giuseppe D, Vianello G, Vittori Antisari L (2014) Multiproxy investigation of a Holocene  
7 sedimentary sequence near Ferrara (Italy): clues on the physiographic evolution of the eastern Padanian plain. J  
8  
9 Soils Sediments 14: 230-242  
10  
11  
12  
13  
14 Blackwell PG, Buck CE, Reimer P (2006) Important features of the new radiocarbon calibration curves. Quaternary Sci  
15  
16 Rev 25:408-413  
17  
18  
19  
20 Boccaletti M., Corti G., Martelli L., 2011. Recent and active tectonics of the external zone of the northern Apennines  
21  
22 (Italy). Int Jour Earth Sci (Geol Rundschau) 100: 1331-1348  
23  
24  
25  
26 Bordon A, Peyron O, Lézine A, Brewer S, Fouache E. (2009) Pollen-inferred Late-Glacial and Holocene climate in  
27  
28 southern Balkans (Lake Maliq). Quatern Int 200: 19-30  
29  
30  
31  
32  
33  
34 Branch NP, Marini NAF (2014) Mid-Late Holocene environmental change and human activities in the northern  
35  
36 Apennines, Italy. Quatern Int 353: 34-51  
37  
38  
39  
40 Bronk Ramsey C (2001) Development of the Radiocarbon Program OxCal. Radiocarbon 43: 355-363  
41  
42  
43  
44 Calcagnile L, Quarta G, D'Elia M (2005) High resolution accelerator-based mass spectrometry: precision accuracy and  
45  
46 background. Appl Radiat Isotopes 62: 623-629  
47  
48  
49  
50 Clark RL (1982) Point count estimation of charcoal in pollen preparations and thin sections of sediment. Pollen et  
51  
52 spores 24: 523-525  
53  
54  
55  
56  
57  
58  
59  
60  
61

- 1  
2  
3  
4  
5  
6  
7  
8  
9  
10  
11  
12  
13  
14  
15  
16  
17  
18  
19  
20  
21  
22  
23  
24  
25  
26  
27  
28  
29  
30  
31  
32  
33  
34  
35  
36  
37  
38  
39  
40  
41  
42  
43  
44  
45  
46  
47  
48  
49  
50  
51  
52  
53  
54  
55  
56  
57  
58  
59  
60  
61  
62  
63  
64  
65
- Clark JS, Patterson WA III (1997) Background and local charcoal in sediments: scales of fire evidence in the paleorecord. Clark, J. S., H. Cachier, J. G. Goldammer & B. Stocks (eds.) *Sediment Records of Biomass Burning and Global Change*. NATO ASI Series 1: Global Environmental Change, 51, Springer (Berlin): 23–48
- Combourieu-Nebout N, Peyron O, Dormoy I, Desprat S, Beaudouin C, Kotthoff U, Marret F. (2009) Rapid climatic variability in the west Mediterranean during the last 25 000 years 25 from high resolution pollen data, *Clim Past* 5: 503–521
- Cremaschi M (1987) Paleosols and vetusols in the central Po Plain (Northern Italy). a study in Quaternary geology and soil development. Unicopli, Milano, pp 306
- Cremaschi M, Nicosia C (2012) Sub-Boreal aggradation along the Apennine margin of the Central Po Plain: geomorphological and geoarchaeological aspects. *Geomorphologie* 2: 155-174.
- Cremonini S, Lorito S, Vianello G, Vittori Antisari L, Fusco F (2007) Suoli olocenici sepolti nel centro urbano di Bologna. Prime considerazioni pedologiche e radiometriche. *Boll Società Italiana della Scienza del Suolo* 56: 48-56
- Cremonini S, Falsone G, Marchesini M, Vinello G, Vittori Antisari L, 2012. Suoli olocenici sepolti nell'Emilia orientale - Holocene buried soils in Eastern Emila Region. *EQA (Environmental Quality-Qualità ambientale) Book 1*: 107-121. (ISSN 2039-9898).
- Cremonini S (2014) La transizione geomorfologica “catena-pianura” nella città di Bologna. Osservazioni per un’analisi evolutiva dell’areale del santuario etrusco di Villa Cassarini nell’arco cronologico pre-protostorico e classico. In Romagnoli S (ed.), *Il santuario etrusco di Villa Cassarini a Bologna*, Bonomia University Press: pp 34-58
- Denefle M, Lezine AM, Fouache E, Dufaure JJ (2000) A 12 000 yr pollen record from Lake Maliq, Albania. *Quaternary Res* 54: 423–432



- Desprat S, Combourieu-Nebout N, Essallami L., Sicre M A, Dormoy I, Peyron O, Siani G, Bout Roumazeilles V, Turon J (2013) Deglacial and Holocene vegetation and climatic changes in the southern Central Mediterranean from a direct land-sea correlation. *Clim Past* 9: 767-787
- Diamond J (2005) *Collapse: how societies Choose to fail or succeed*. Viking Pres, New York, pp 137- 155
- Di Giuseppe D, Bianchini G, Faccini B, Coltorti M. (2014) Combination of wavelength dispersive X-ray fluorescence analysis and multivariate statistic for alluvial soils classification: A case study from the Padanian Plain (Northern Italy). *X-Ray Spectrometry* 43: 165-174
- Facchinelli A, Sacchi E, Mallen L (2001) Multivariate statistical and GIS approach to identify heavy metal sources in soils. *Environ Pollut* 114: 313-324
- Faegri K, Iversen J (1989) *Textbook of Pollen Analysis*, 4th edition. Chichester, John Wiley & sons, pp 328
- Farabegoli E, Rossi Pisa P, Costantini B, Gardi C (1994) Cartografia tematica per lo studio dell'erosione a scala di bacino. *Rivista di Agronomia* 28: 356-363.
- Fleitmann D, Burns S J, Mangini A, Mudelsee M, Kramers J, Villa I, Neff U, Al-Subbary AA, Buettner A, Hippler D, Matter A (2007) Holocene ITCZ and Indian monsoon dynamics recorded in stalagmites from Oman and Yemen (Socotra), *Quaternary Sci Rev* 26: 170-188
- Fletcher WJ, Sanchez Goñi MF, Peyron O, Dormoy I (2010) Abrupt climate changes of the last deglaciation detected in a Western Mediterranean forest record. *Clim Past* 6: 245-264
- Fiorentino G, Caracuta V, Calcagnile L, D'Elia M, Matthiae P, Mavelli F, Quarta G (2008) Third millennium B.C. climate change in Syria highlighted by carbon stable isotope analysis of <sup>14</sup>C-AMS dated plant remains from Ebla. *Palaeogeogr Palaeoclimatol* 266: 51-58
- Fontana F, Moncel M-H, Nenzioni G, Onorevoli G, Peretto C, Combier J (2013) Widespread diffusion of technical innovations around 300,000 years ago in Europe as a reflection of anthropological and social transformations?

New comparative data from the western Mediterranean sites of Orgnac (France) and Cave dall'Olio (Italy). *J*

*Anthropol Archaeol* 32: 478-498

Frisia S, Borsato A, Spotl C, Villa I, Cucchi F (2005) Climate variability in the SE Alps of Italy over the past 17000 years reconstructed from a stalagmite record. *Boreas* 34: 445–455

Gasperi G, Cremaschi M, Mantovani Uguzzoni MP., Cardarelli A, Cattani M, Labate D (1989) Evoluzione plio-  
quaternaria del margine appenninico modenese e dell'antistante pianura. Note illustrative alla carta geologica.  
*Mem Soc Geol It* 29: 375-431

Gee GW, Bauder JW (1986) Particle-size analysis. In: Klute A. (ed.), *Methods of Soil Analysis, Part 1, Second edition.*  
Number 9 of the series *Agronomy*. ASA and SSSA, Madison WI, USA, pp 383-411

Giraudi C, Magny M, Zanchetta G, Drysdale RN (2011) The Holocene climatic evolution of Mediterranean Italy: A  
review of the continental geological data. *The Holocene* 21: 105–115

Grosser D (1977) *Die Holzer Mitteleuropas. Ein Mikrophotographischer Lehratlas.* Springer, Berlin, New York,  
Heidelberg, Tokyo.

Hather JG (2000) *The identification of the Northern European Woods. A guide for archaeologists and conservators.*  
Archetype Publications, London

Jacquot C, Trenard Y, Dirol D (1973) *Atlas d'anatomie des bois d'Angiospermes. vol 1–2.* Centre Technique du bois,  
Paris

Joannin S, Vanniere B., Galop D, Peyron O, Haas JN, Gilli A, Chapron E., Wirth SB, Anselmetti F, Desmet M, Magny  
M (2013) Climate and vegetation changes during the Lateglacial and early-middle Holocene at Lake Ledro  
(southern Alps, Italy). *Clim Past* 9: 913-933

Jolliffe IT (2002) *Principal Component Analysis,* Springer, New York, 488 pp

- 1  
2  
3  
4  
5  
6  
7  
8  
9  
10  
11  
12  
13  
14  
15  
16  
17  
18  
19  
20  
21  
22  
23  
24  
25  
26  
27  
28  
29  
30  
31  
32  
33  
34  
35  
36  
37  
38  
39  
40  
41  
42  
43  
44  
45  
46  
47  
48  
49  
50  
51  
52  
53  
54  
55  
56  
57  
58  
59  
60  
61
- Kotthoff U, Pross, J, Muller UC, Peyron O, Schmiedl G, Schulz H (2008) Climate dynamics in the borderlands of the Aegean Sea during formation of Sapropel S1 deduced from a marine pollen record. *Quaternary Sci Rev* 27: 832-845
- Lenzi F, Nenzioni G, 1996. Lettere di pietra. I depositi pleistocenici: sedimenti, industrie e faune del margine appenninico bolognese. Bologna, 1-867.
- Loeppert RH, Suarez DL (1996) Carbonate and gypsum. In: Sparks D.L. (ed.), *Method of Soil Analysis. Part 3, Chemical Methods*. SSSA and ASA, Madison, pp 437–474
- Lowe JJ, Accorsi AC, Bandini Mazzanti M, Bishop A, Van der Kaars S, Forlani L, Mercuri AM, Rivalenti C, Torri P, Watson (1996) Pollen stratigraphy of sediment sequences from crater lakes Albano and Nemi (near Rome) and from the central Adriatic, spanning the interval from oxygen isotope Stage 2 to the present day. *Memorie Istituto Italiano Idrobiologia* 55:71-98
- Magny M, De Beaulieu JL, Drescher-Schneider R, Vanniere B, Walter-Simonnet AV, Millet L, Bossuet G, Peyron O (2006) Climatic oscillations in central Italy during the Last Glacial-Holocene transition: the record from Lake Accesa, *J Quaternary Sci* 21: 311–320
- Magri D, Sadori L (1999) Late Pleistocene and Holocene pollen stratigraphy at Lago di Vico (central Italy). *Veget Hist Archaeobot* 8 247-260
- Martelli L, Amorosi A, Severi P, (2009) Note illustrative della Carta Geologica d'Italia alla scala 1:50.000. Foglio 221-Bologna, Roma, 127 pp
- Meier HA, Driese SG, Nordt LC, Forman SL, Dworkin SI (2014) Interpretation of Late Quaternary climate and landscape variability based upon buried soil macro- and micromorphology, geochemistry, and stable isotopes of soil organic matter, Owl Creek, central Texas, USA. *Catena* 114: 157-168
- Miller GH, Brigham-Grette, J, Alley RB, Anderson L, Bauch HA, Douglas MSV, Edwards ME, Elias SA, Finney BP, Fitzpatrick JJ, Funder SV, Herbert TD., Hinzman LD, Kaufman DS, MacDonald GM, Polyak L, Robock A,

Serreze MC, Smol JP, Spielhagen R, White JWC., Wolfe AP, Wolff EW (2010) Temperature and precipitation history of the Arctic. *Quaternary Sci Rev*: 29, 1679-1715

Moore PD, Webb JA, Collinson ME (1991) *Pollen Analysis*, 2nd edition, Blackwell, Oxford

Muttoni G, Scardia G, Kent DV, Morsiani E, Tremolada F, Cremaschi M, Peretto C (2011) First dated human occupation of Italy at ~0.85 Ma during the late Early Pleistocene climate transition. *Earth Planet Sci Lett* 307: 241-252.

Nenzioni G (1985) Testimonianze mesolitiche, neolitiche e dell'età del Rame dal territorio di S. Lazzaro di Savena. In Lenzi F., Nenzioni G., Peretto C (Eds), *Materiali e documenti per un museo della preistoria. S. Lazzaro di Savena e il suo territorio*, Bologna, 211-250

Natali C, Bianchini G (2015) Thermally based isotopic speciation of carbon in complex matrices: a tool for environmental investigation. *Environ Sci Pollut Res*, in press (DOI 10.1007/s11356-015-4503-x)

Orombelli G, Ravazzi C (1996) The Late Glacial and Early Holocene: chronology and paleoclimate. *Il Quaternario* 9: 439-444

Patterson WA III, Edwards KJ, MacGuire DJ (1987) Microscopic charcoal as a fossil indicator of fire. *Quat Sci Rev* 6: 3-23

Picotti V, Bertotti G, Capozzi R, Fesce AM (1997) Evoluzione tettonica quaternaria della pianura padana centro-orientale e dei suoi margini. *Il Quaternario* 19: 513-520.

Picotti V., Pazzaglia FJ (2008). A new active tectonic model for the construction of the Northern Apennines mountain front near Bologna (Italy). *J Geophys Res* 113: B08412

Pignatti S (1982) *Flora d'Italia*, Edagricole, Bologna

- 1 Ravazzi C, Donegana M, Vescovi E, Arpentì E, Caccianiga M, Kaltenrieder P, Londeix L, Marabini S, Mariani S, Pini  
2 R, Vai GB, Wick L (2006) A new Late-glacial site with *Picea abies* in the northern Apennine foothills: an  
3 exception to the model of glacial refugia of trees. *Veget Hist Archaeobot* 15: 357-371  
4  
5  
6 Ravazzi C, Deaddis M, De Amicis M, Marchetti M, Vezzoli G, Zanchi A (2012) The last 40 ka evolution of the Central  
7 Po Plain between the Adda and Serio rivers. *Geomorphologie* 2: 131-154.  
8  
9  
10  
11  
12 Rottoli M, Castiglioni E (2009) Prehistory of plant growing and collecting in Northern Italy, based on seed remains  
13 from the Early Neolithic to the Chalcolithic (c. 5600 - 2100 cal B.C.). *Veget Hist Archaeobot* 18: 91-103  
14  
15  
16  
17  
18 Rudnick RL, Gao S (2014) Composition of the Continental Crust. *Treatise on Geochemistry (Second Edition)* 4: 1-51  
19  
20  
21  
22  
23 Scarani R (1963) Repertorio di scavi e scoperte dell'Emilia e Romagna, in: "Preistoria dell'Emilia e Romagna" vol. 2,  
24 175 -617, Bologna.  
25  
26  
27  
28  
29 Schoeneberger PJ, Wysocki DA, Benham EC, and Soil Survey Staff (2012) Field book for describing and sampling  
30 soils. Version 3.0. Natural Resources Conservation Service. National Soil Survey Center. Lincoln. NE  
31  
32  
33  
34  
35 Schweingruber FH (1990) Anatomie europäischer Hölzer. Eidgenössische Forschungsanstalt für Wald, Schnee und  
36 Landschaft, Birmensdorf (ed.). Verlag Paul Haupt, Bern u. Stuttgart: 800 pp  
37  
38  
39  
40  
41  
42  
43 Soil Survey Staff (2014) Keys to Soil Taxonomy, 12th ed. USDA-Natural Resources Conservation Service, Washington,  
44 DC  
45  
46  
47  
48  
49 Stramondo S, Saroli M, Tolomei C, Moro M, Doumaz F, Pesci A, Loddo F, Baldi P, Boschi E (2007) Surface  
50 movements in Bologna (Po plain – Italy) detected by multitemporal DInSAR. *Remote Sens Environ* 110: 304-316.  
51  
52  
53  
54  
55 Stuiver M, Polach HA (1977) Discussion: reporting of <sup>14</sup>C data. *Radiocarbon* 19: 355-363  
56  
57  
58  
59  
60  
61

- 1  
2  
3  
4 Tutin TG, Heywood VH, Burges NA, Moore DM, Valentine DH, Walters SM, Webb DA (eds.) 1964–1993. *Flora*  
5 *Europaea*, Vols 2–5 and Vol. 1, 2nd edn. Cambridge University Press, Cambridge, UK  
6  
7  
8  
9  
10 Vescovi E, Ammann B, Ravazzi C, Tinner W (2010) A new Late-Glacial and Holocene record of vegetation and fire  
11 History from Lago del Greppo, Northern Apennines, Italy. *Veg Hist Archaeobot* 19: 219–233  
12  
13  
14  
15  
16 Vittori Antisari L, Cremonini S, Desantis P, Vianello G (2011). Anthropogenic cycles in a chronosequence from the  
17 bronze age to renaissance period (Bologna, Italy). *EQA* 6: 1–6  
18  
19  
20  
21  
22 Vittori Antisari L, Cremonini S, Desantis P, Calastri C, Vianello G (2013) Chemical characterisation of anthro-  
23 technosols from Bronze to Middle Age in Bologna (Italy). *J Archaeol Sci* 40: 3660–3671.  
24  
25  
26  
27 von Grafenstein U, Eicher U, Erlenkeuser H, Ruch P, Schwander J, Ammann B (2000) Isotope signature of the Younger  
28 Dryas and two minor oscillations at Gerzensee (Switzerland): palaeoclimatic and palaeolimnologic interpretation  
29 based on bulk and biogenic carbonates. *Palaeogeogr Palaeoclimatol Palaeoecol* 159: 215–229.  
30  
31  
32 Yu S, Colman SM, Lowell TV, Milne GA, Fisher TG, Breckenridge A, Boyd M, Teller JT (2010) Freshwater outburst  
33 from Lake Superior as a trigger for the cold Event 9300 Years Ago. *Science*, 328, 1262–1266  
34  
35  
36  
37 Watts W A, Allen JRM, Huntley B (1996). Vegetation history and palaeoclimate of the Last Glacial period at Lago  
38 Grande di Monticchio, southern Italy, *Quaternary Sci Rev* 15: 133–53  
39  
40  
41  
42  
43 Wiersma AP, Jongma JI (2010) A role for icebergs in the 8.2 ka climate event. *Clim Dynam* 35: 535–549  
44  
45  
46  
47 Whitlock C, Larsen C (2001) Charcoal as a fire proxy. J. P. Smol, H. J. B. Birks & W. M. Last (eds.), *Tracking*  
48 *Environmental Change Using Lake sediments*, 3 - Terrestrial, Algal, and Siliceous Indicators. Kluwer Academic  
49 Publishers, Dordrecht, The Netherlands  
50  
51  
52  
53  
54  
55 Whitlock C, Millspaugh SH (1996) Testing assumptions of fire history studies: an examination of modern charcoal  
56 accumulation in Yellowstone National Park. *The Holocene*, 6: 7–15  
57  
58  
59  
60  
61  
62  
63  
64  
65

Zanchetta G, Giraudi C, Sulpizio R, Magny M, Drysdale RN, Sadori L (2012) Constraining the onset of the Holocene “Neoglacial” over the central Italy using tephra layers. *Quaternary Res* 78: 236–247

## Figure captions

**Figure 1.** A) Geomorphological outline of the S. Lazzaro di Savena surroundings and related foothill. B) Geological and pedological outline of the same area.

**Figure 2.** Stratigraphic log, soil and horizon sequence coupled with selected chemical parameters of the studied site.

**Figure 3.** Box plot showing textural and physicochemical parameters of the different pedostratigraphic sets: I includes samples 1,2,3,4,5; II includes samples 6,7,8,9 10; III includes samples 11,12 13; IV includes samples 14 and 15.

**Figure 4.** XRD analyses of soil samples representative of three excavation levels. Note that the more superficial sample 1 records only quartz (preponderant) and feldspar (subordinate), whereas deeper levels (6 and 12 samples) also record the presence of clay minerals. Calcite seems abundant only in the deeper horizons.

**Figure 5.** 3D plots of F1-F2-F3 discriminating factors obtained by the statistical elaboration of the X-ray fluorescence (XRF) geochemical data.

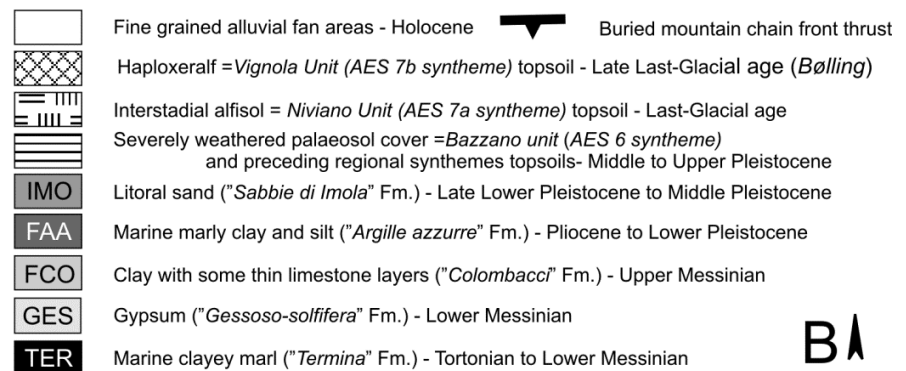
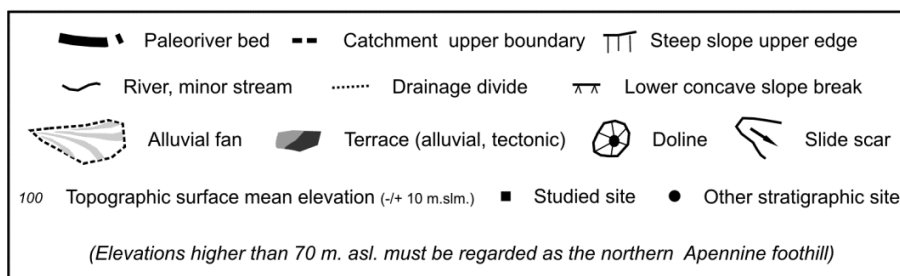
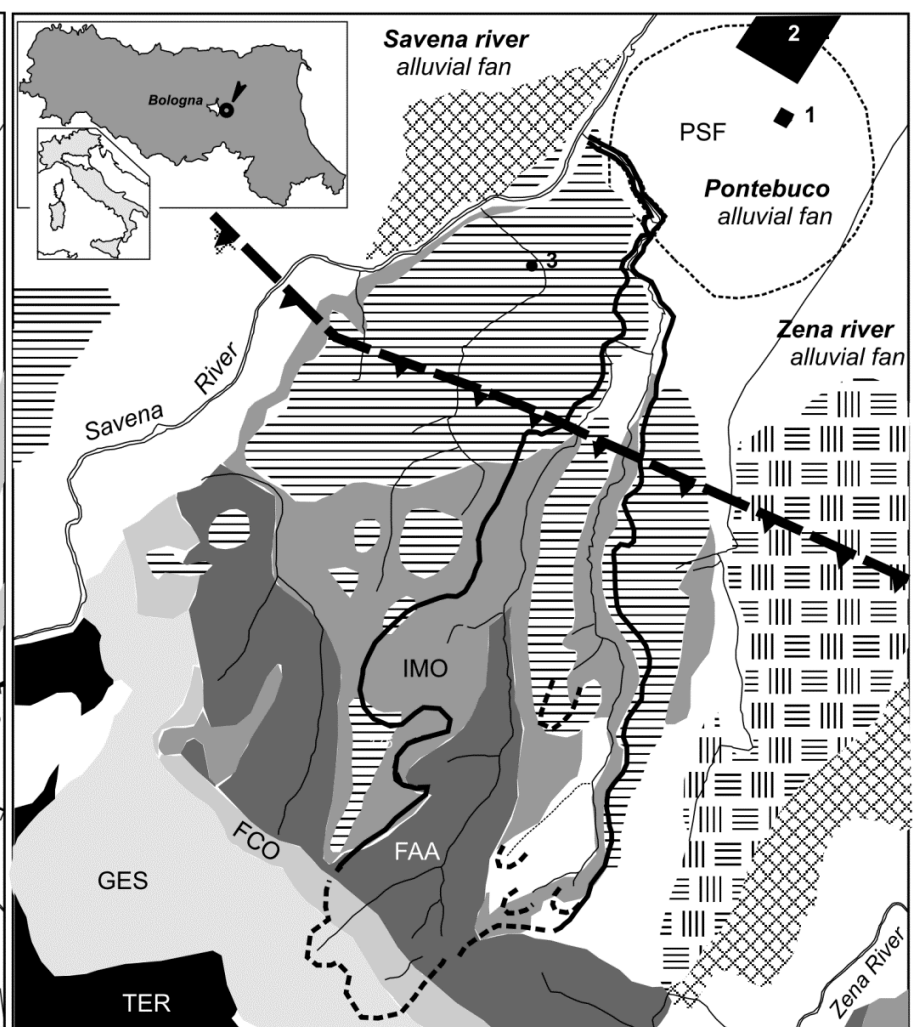
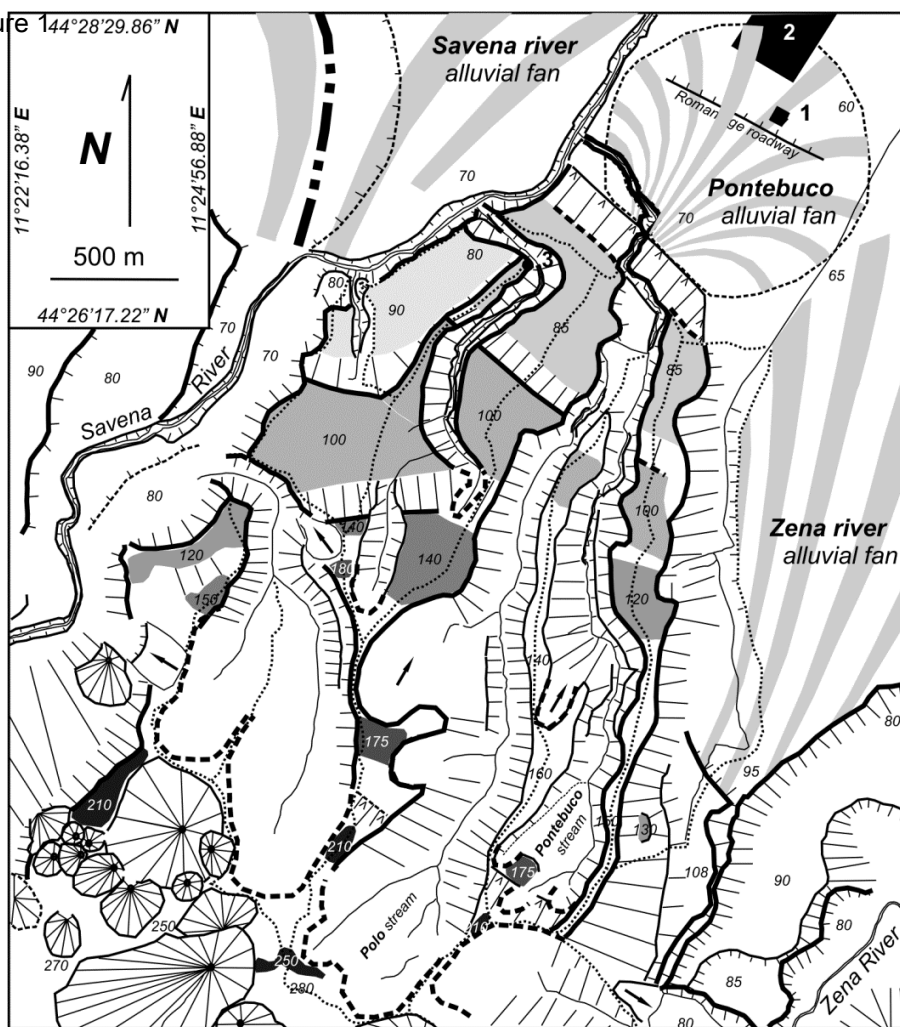
**Figure 6.** Trace element content vs depth. The elements have been grouped according to their geochemical affinity and normalized to the UCC (Upper Continental Crust Composition; Rudnick and Gao, 2014).

**Figure 7.** *Stratigraphic variation of  $\delta^{13}\text{C}$  of the total C budget and  $\delta^{13}\text{C}$  organic C fraction. The first parameter highlights the horizons containing significant amount of carbonate, whereas the second parameter gives indication on the nature of the existing vegetation that generated the organic matter.*

1  
2  
3  
4  
5  
6  
7  
8  
9  
10  
11  
12  
13  
14  
15  
16  
17  
18  
19  
20  
21  
22  
23  
24  
25  
26  
27  
28  
29  
30  
31  
32  
33  
34  
35  
36  
37  
38  
39  
40  
41  
42  
43  
44  
45  
46  
47  
48  
49  
50  
51  
52  
53  
54  
55  
56  
57  
58  
59  
60  
61  
62  
63  
64  
65



Figure 144°28'29.86" N



A

B

Figure 2

[Click here to download Figure: Fig 2 - S Lazzaro - 1 Maggio 2015 B.tif](#)

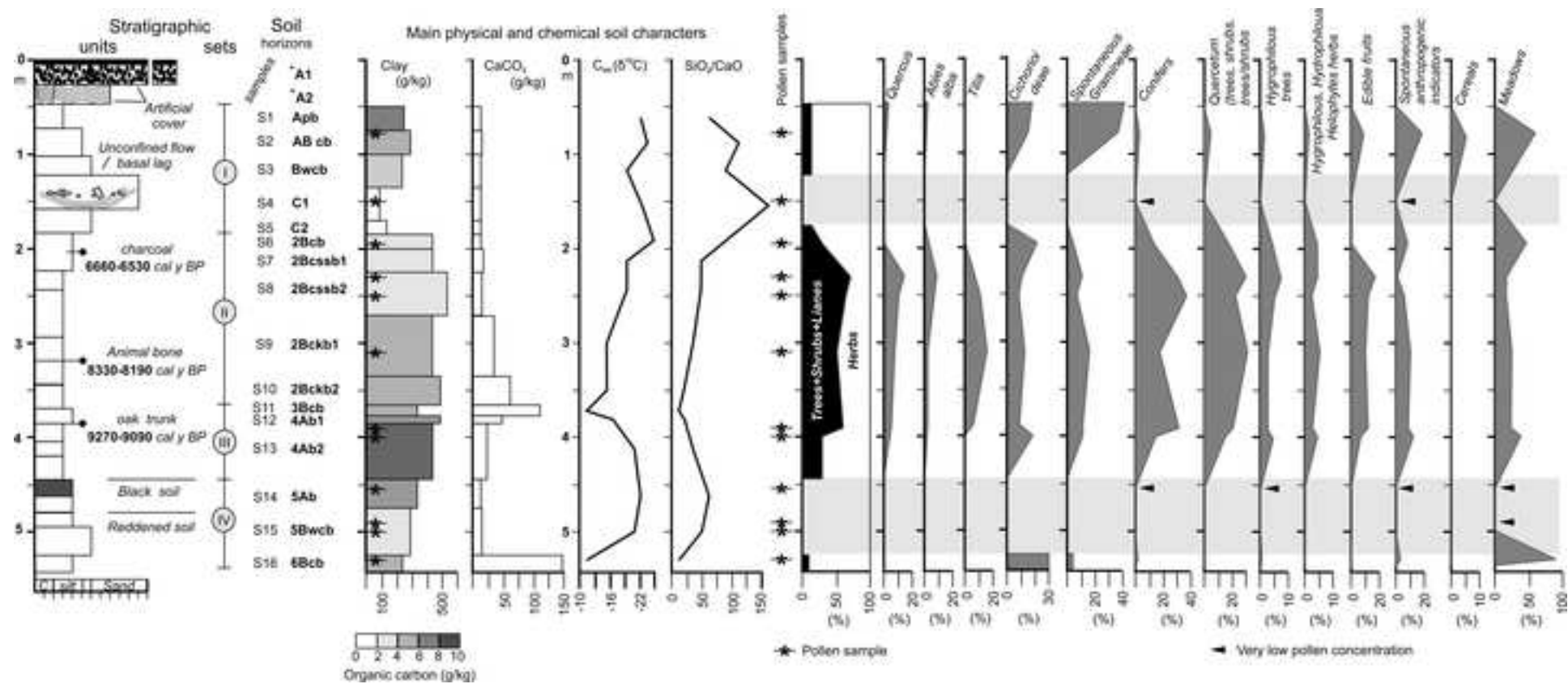


Figure 3  
[Click here to download Figure: SLAZ Figure 3.tif](#)

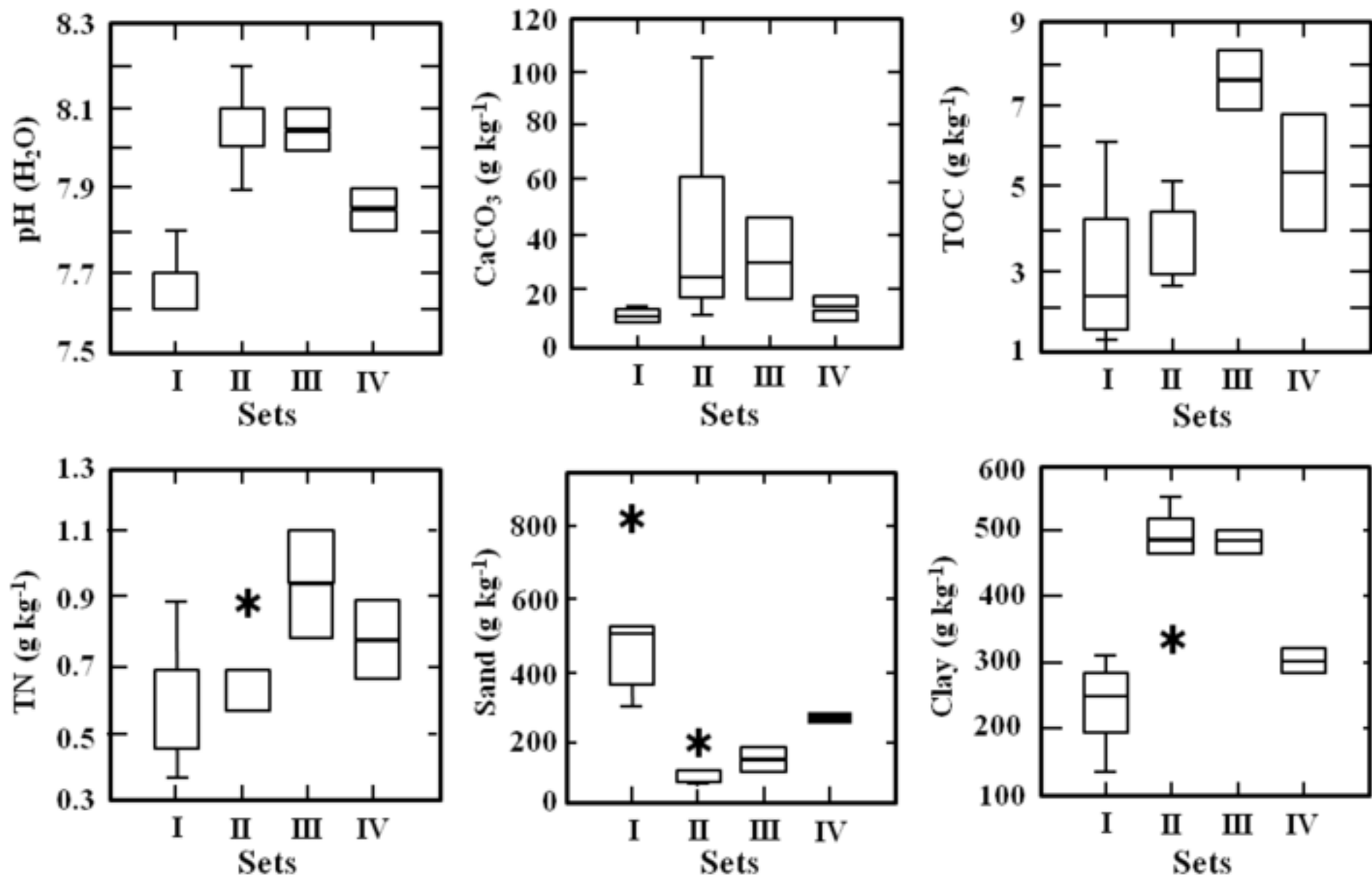


Figure 4  
[Click here to download Figure: SLAZ Figure 4.tif](#)

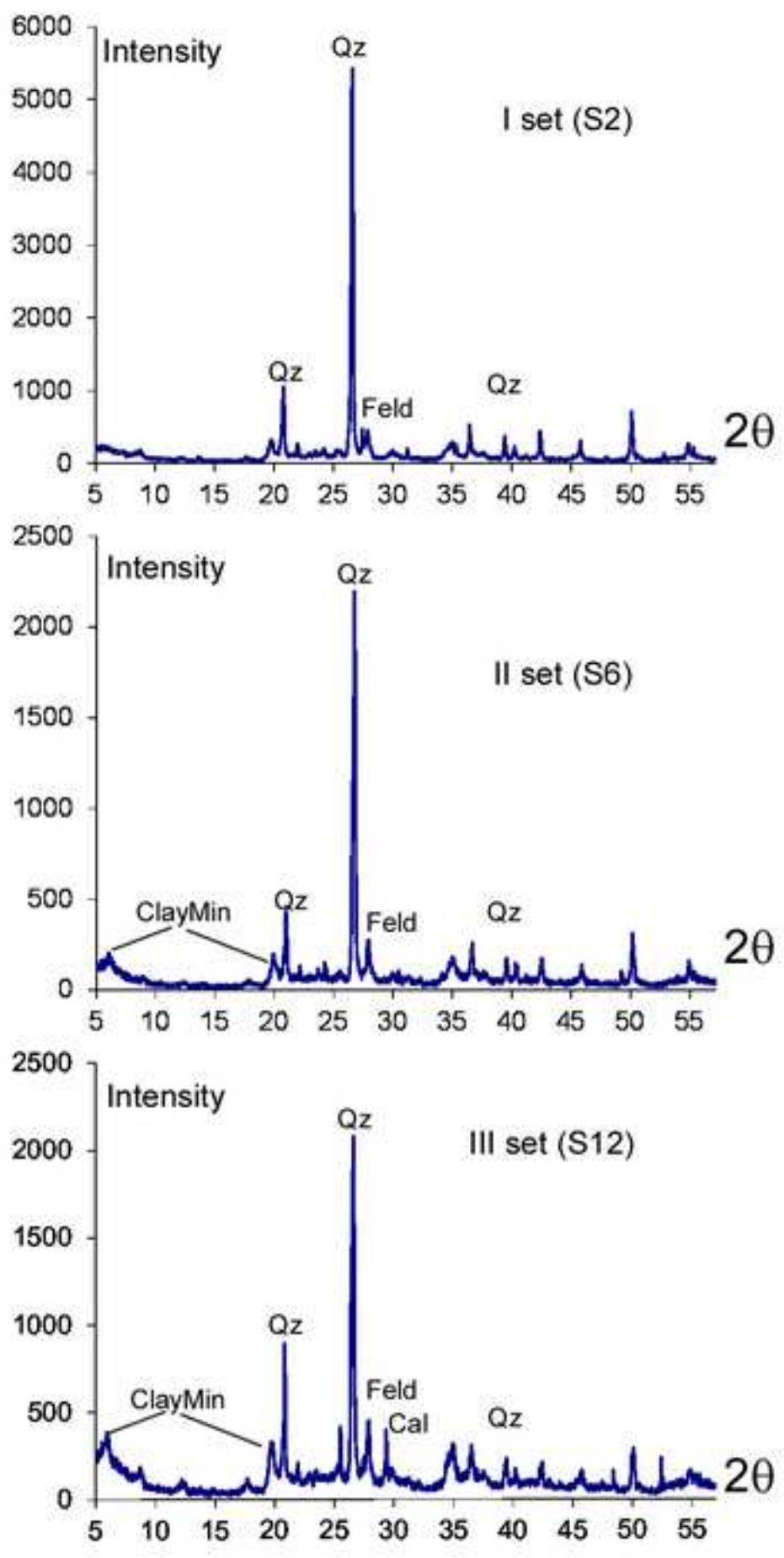


Figure 5  
[Click here to download Figure: SLAZ Figure 5.tif](#)

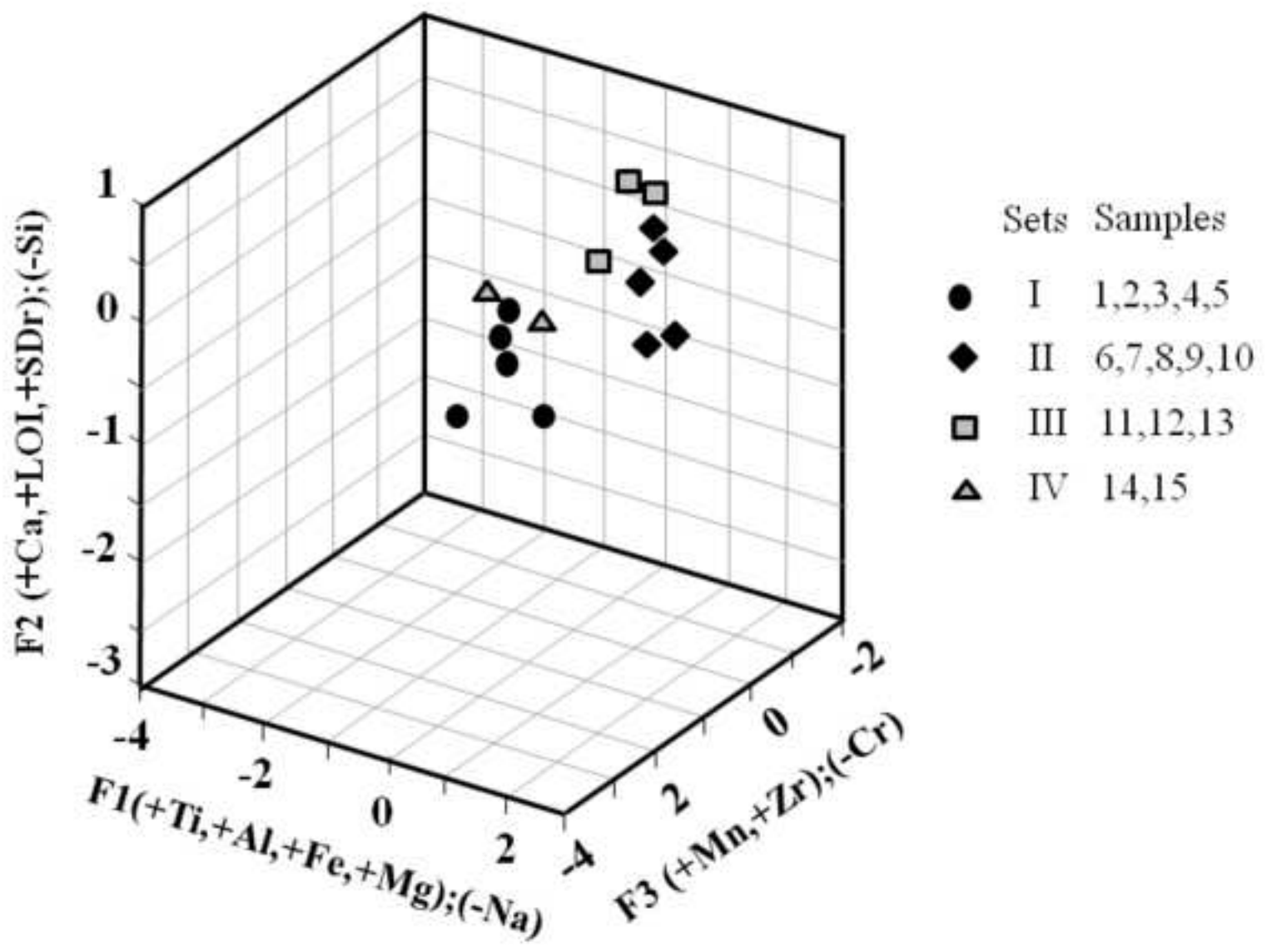


Figure 6  
[Click here to download Figure: SLAZ Figure 6.tif](#)

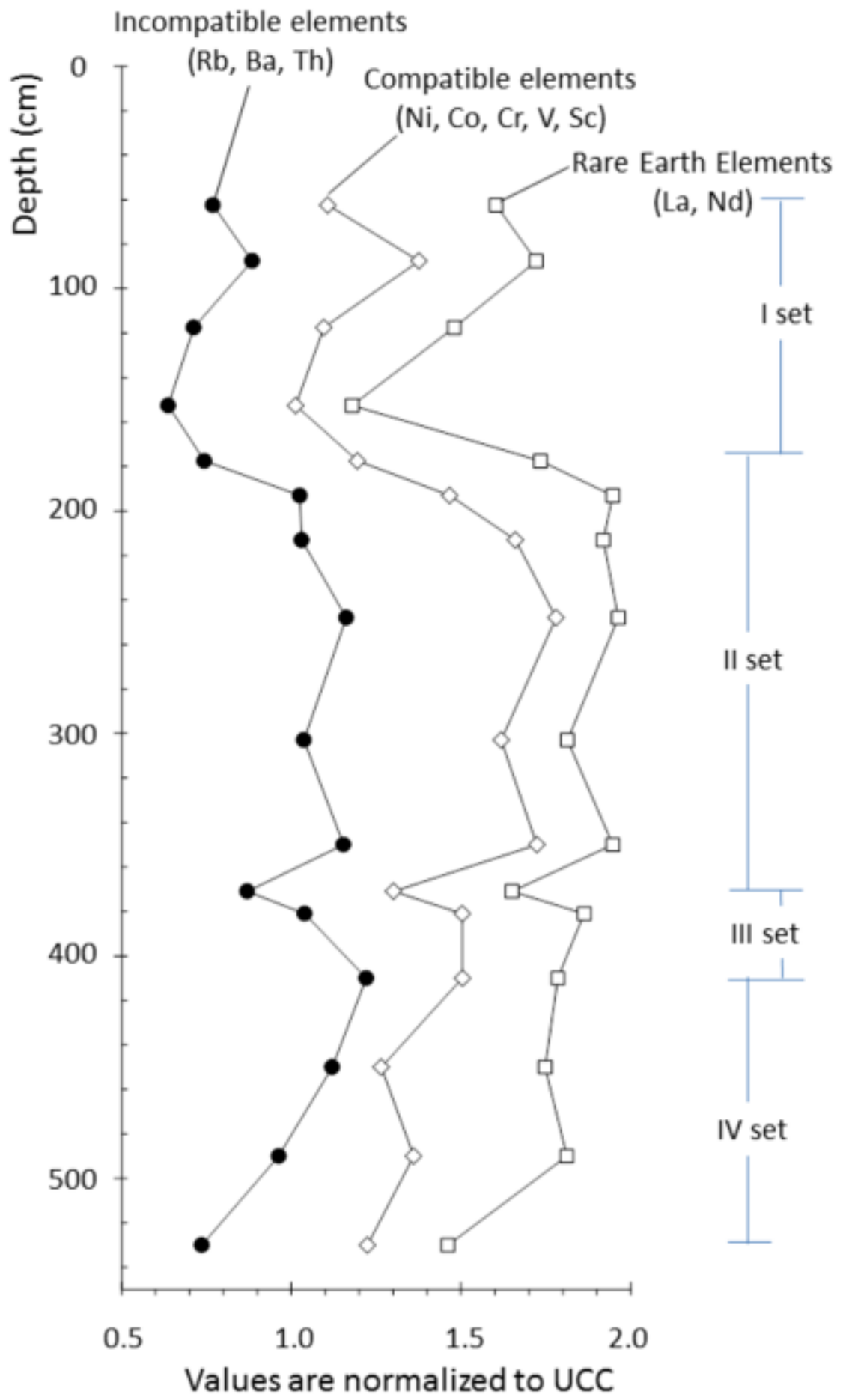
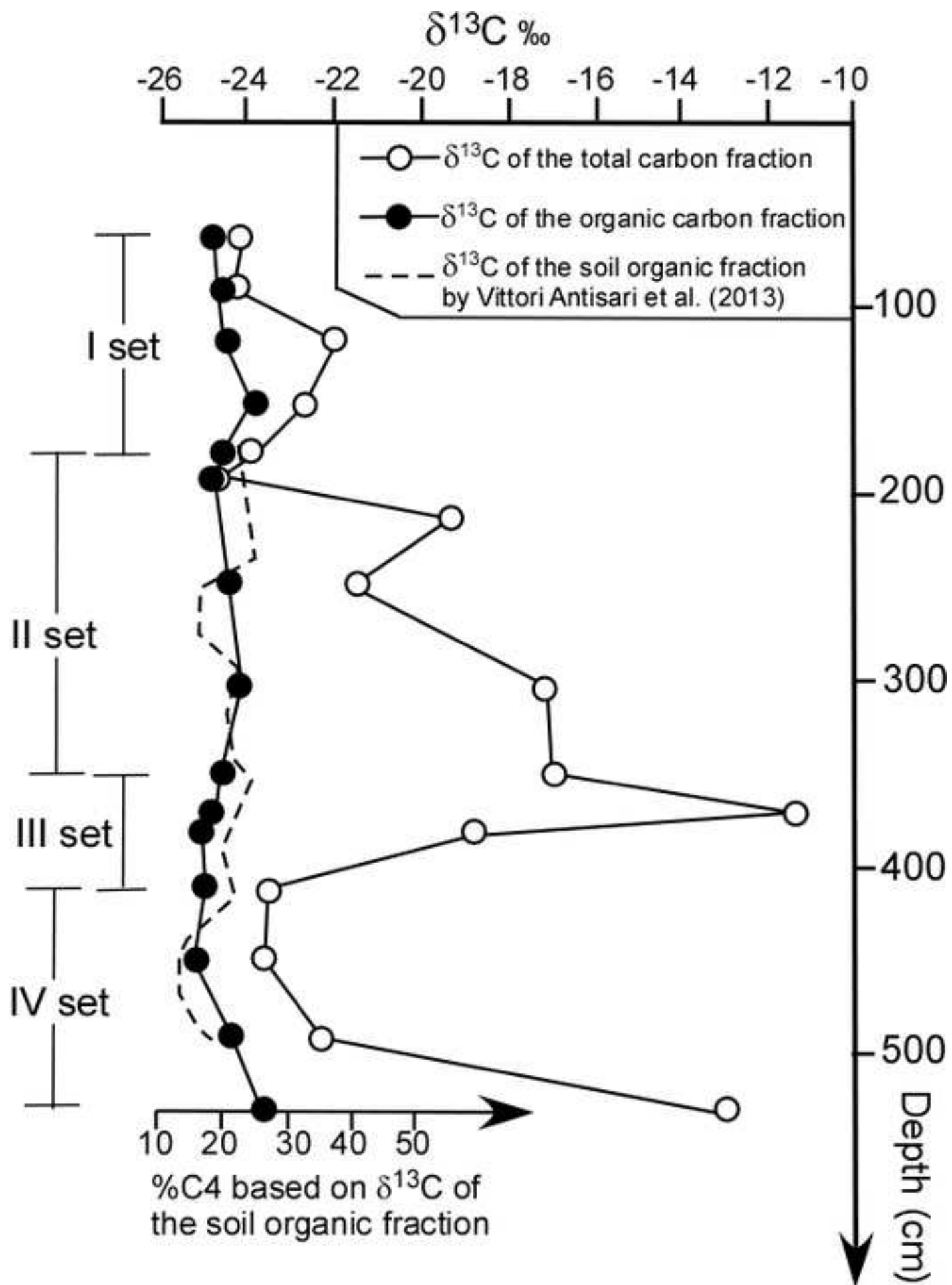


Figure 7  
Click here to download Figure: SLAZ Figure 7.tif



**Table 1** – Main descriptive elements of investigated soil profiles. Codes according to Schoeneberger et al. (2012)

Stratigraphic set	Sample	Horizons				Color Munsell		Mottles					Texture	Structure	Consistence	Concentrations	Rock and other fragments				
		Horizon	Depth (cm)	Boundary		dry	moist	Q	S	C	Colour	M					G_S_T	D_M_S_P	Q_S_K	V%	R
				D	T																
	Not collected	^A1	0-30	A	S								SL								
		^A2	30-50	A	S								SL								
	S1	Apb	50-75	C	S	10YR 6/3	10YR 5/3	--	-	-	----	----	L	3_m_pl	SH_FR_(w)ss_(w)ps	-----	1	SR			
	S2	ABcb	75-100	D	S	10YR 6/4	10YR 5/4	vf	1	F	10YR 5/6	d	CL	3_m_pr	SH_FR_(w)ss_(w)ps	f_1_RSB	0	--			
I	S3	Bwcb	100-135	A	S	10YR 6/6	10YR 5/4	f	1	F	10YR 5/6	d	L	3_m_pr	HA_FI_(w)ss_(w)ps	f_1_RSB	2	SR			
	S4	C1	135-170	G	S	10YR 6/6	10YR 6/8	--	-	-	----	-	SL	0_f_sg	SH_FR_(w)so_(w)po	f_1_CBM	50	RO			
	S5	C2	170-185	C	S	10YR 7/4	10YR 6/6	c	1	F	10YR 5/8	d	L	3_m_abk	HA_FI_(w)so_(w)po	f_1_DNN	3	RO			
	S6	2Bcb	185-201	C	S	2.5Y 6/4	2.5Y 4/2	m	1	P	7.5YR 6/8	d	SiC	2_f_abk	VH_FI_(w)ss_(w)vp	c_1_RSB	0	--			
	S7	2Bcssb1	201-225	C	S	2.5Y 6/2	2.5Y 4/2	m	1	D	2.5Y 5/4	d	SiC	2_f_abk	VH_FI_(w)ss_(w)ps	c_1_CAN	0	--			
II	S8	2Bcssb2	225-271	C	S	2.5Y 6/3	2.5Y 4/2	m	3	D	10YR 5/6	d	SiC	2_m_abk	VH_FI_(w)ss_(w)ps	c_1_CAC	0	--			
	S9	2Bckb1	271-335	C	S	2.5Y 5/4	10YR 4/3	c	2	F	5YR 3/2	d	SiC	2_m_abk	VH_FI_(w)s_(w)p	c_2_CAN	2	RO			
	S10	2Bckb2	335-365	A	W	10YR 5/3	10YR 3/3	m	4	D	G 2 8/5B	d	SiC	3_m_pr	HA_VFR_(w)ss_(w)vp	c_1_CAC/SFB	2	RO			
	S11	3Bcb	365-377	A	W	10YR 7/3	10YR 4/3	--	-	-	----	----	SiCL	2_f_abk	HA_FR_(w)vs_(w)ps	c_2_CAM/RSB	2	RO			
III	S12	4Ab1	377-385	C	W	10YR 5/3	10YR 3/3	--	-	-	----	----	SiC	3_m_abk	EH_EF_(w)s_(w)p	c_1_CAC	0				
	S13	4Ab2	385-445	C	W	10YR 4/2	10YR 3/2	--	-	-	----	----	SiC	3_f_abk	VH_VFI_(w)ss_(w)vp	m_2_CAM	0				
	S14	5Ab	445-475	C	W	10YR 3/3	10YR 3/2	f	1	F	10YR 5/6	d	CL	2_f_gr	SH_VFR_(w)so_(w)ps	m_2_CAM	5	SR			
IV	S15	5Bwcb	475-525	C	W	2.5Y 6/6	2.5Y 4/4	m	2	F	10YR 6/8	d	CL	2_m_sbk	HA_VFR_(w)s_(w)vp	m_2_CAN	2	SR			
	S16	6Bcb	525-545		U	2.5Y 6/4	10YR 5/4	f	2	D	10YR 6/8	d	L	2_f_abk	VH_FR_(w)s_(w)p	c_1_CAN	0				

**Horizon Boundary.** (D) Distinctness: A = abrupt, C = clear, G = gradual, D = diffuse (T) Topography: S = smooth, W = wavy, U = unknown

**Mottles.** (Q) Quantity: vf=very few; f=few; c=common; m=many -- (S) Size: 1=fine; 2=medium; 3=coarse; 4=very coarse -- (C) Contrast: F=faint; D=distinct; P=prominent -- (M) Moisture state: d=dry

**Texture.** Field estimation: SL = sandy loam, L = loam, SiCL=silty clay loam; SiC = silty clay; CL = clay loam.

**Structure.** (G) Grade: 0 = structureless/very weak; 1 = weak; 2 = moderate; 3 = strong -- (S) Size: vf = very fine; f = fine; m = medium; c = coarse -- (T) Type: gr = granular, abk = angular blocky, sbk = subangular blocky; pr = prismatic; pl = plat; sg = single grain.

**Consistence.** Rupture resistance: (D) Dry: SH = slightly hard; HA=hard; VH=very hard; EH=extremely hard -- (M) Moist: VFR = very friable; FR=friable; FI=firm; VFI=very firm; EF=extremely firm -- (S) Stickiness: (w)so = non-sticky, (w)ss = slightly sticky, (w)s = moderately sticky ; (w)vs=very sticky -- (P) Plasticity: (w) po = non-plastic, (w) ps = slightly plastic, (w)p = moderately plastic; (w)vp=very plastic

**Concentrations.** (Q) Quantity: f= few; c= common; m = many -- (S) Size: 1 = fine; 2 = medium; 3= coarse -- (K) Kind: . CAC = carbonate concretions; CAM = carbonate masses; CAN = carbonate nodules; CBM = clay bodies; DNN = durinodes-SiO<sub>2</sub>; RSB = root sheaths; SFB = shell fragments

**Rock and other fragments.** (K) Kind: SHF = shell (V%) Fragment content % by volume -- (R) Roundness: SR =subrounded; RO= rounded



**Table 2.** *Chemical-physical characters of the investigated soil profiles*

Stratigraphic set	Sample	Horizon	Depth cm	pH (H <sub>2</sub> O)	EC mS/cm 20°C	Texture					CaCO <sub>3</sub>	TOC	TN
						Sand G	Sand F	Silt G	Silt F	Clay			
I	S1	Apb	50-75	7.6	207	87	268	132	264	249	9	6.2	0.9
	S2	ABcb	75-100	7.7	142	60	222	94	328	296	11	4.1	0.7
	S3	Bwcb	100-135	7.7	197	140	347	109	173	231	9	2.4	0.5
	S4	C1	135-170	7.8	164	526	280	33	51	109	10	1.4	0.4
	S5	C2	170-185	7.6	135	124	372	157	170	177	9	1.6	0.5
II	S6	2Bcb	185-201	7.9	157	16	95	99	338	452	11	4.8	0.9
	S7	2Bcssb1	201-225	8.0	240	26	80	53	381	460	18	3.0	0.6
	S8	2Bcssb2	225-271	8.1	240	15	56	39	365	525	18	3.6	0.6
	S9	2Bckb1	271-335	8.0	244	10	70	44	400	475	33	4.3	0.9
	S10	2Bckb2	335-365	8.0	274	31	51	21	393	503	60	5.2	0.7
III	S11	3Bcb	365-377	8.2	263	41	145	176	312	326	103	4.1	0.6
	S12	4Ab1	377-385	8.1	243	14	96	86	332	472	46	6.8	0.8
	S13	4Ab2	385-445	8.0	243	9	142	113	287	449	19	8.3	1.1
IV	S14	5Ab	445-475	7.8	216	9	241	183	269	297	10	6.7	0.9
	S15	5Bwcb	475-525	7.9	215	20	233	204	271	271	15	4.0	0.7
	S16	6Bcb	525-545	8.2	235	58	230	183	289	240	153	4.1	0.7

**Table 3.** Concentration of major and trace elements obtained by XRF

Sample	Horizon	Depth cm	SiO <sub>2</sub>	TiO <sub>2</sub>	Al <sub>2</sub> O <sub>3</sub>	Fe <sub>2</sub> O <sub>3</sub>	MnO	MgO	CaO	Na <sub>2</sub> O	K <sub>2</sub> O	P <sub>2</sub> O <sub>5</sub>	LOI	
			%											
I	S1	Apb	50-75	67.81	0.63	14.14	6.33	0.13	1.81	0.94	1.05	2.67	0.28	4.21
	S2	ABcb	75-100	65.47	0.70	15.75	7.31	0.16	2.03	0.61	0.93	2.86	0.11	4.07
	S3	Bwcb	100-135	69.93	0.53	14.38	5.59	0.11	1.55	0.72	1.20	2.82	0.09	3.09
	S4	C1	135-170	77.89	0.29	10.59	4.14	0.09	0.78	0.38	1.28	2.75	0.09	1.72
	S5	C2	170-185	69.99	0.60	14.19	6.02	0.16	1.60	0.65	1.21	2.76	0.09	2.74
II	S6	2Bcb	185-201	61.06	0.79	17.53	8.58	0.07	2.36	1.02	0.68	2.60	0.07	5.24
	S7	2Bessb1	201-225	59.32	0.78	17.46	8.69	0.12	2.50	1.70	0.63	2.59	0.07	6.14
	S8	2Bessb2	225-271	57.93	0.80	17.86	9.32	0.11	2.68	1.43	0.56	2.70	0.08	6.53
	S9	2Bckb1	271-335	57.49	0.80	17.30	8.94	0.10	2.65	2.27	0.59	2.68	0.10	7.09
	S10	2Bckb2	335-365	55.35	0.78	17.37	8.92	0.11	2.71	3.02	0.52	2.82	0.11	8.27
III	S11	3Bcb	365-377	55.14	0.73	15.83	7.27	0.10	2.36	6.07	0.69	2.79	0.13	8.89
	S12	4Ab1	377-385	55.43	0.78	17.67	8.67	0.10	2.68	3.00	0.55	3.11	0.15	7.85
	S13	4Ab2	385-445	58.15	0.77	17.77	8.53	0.11	2.68	1.57	0.63	3.18	0.13	6.48
IV	S14	5Ab	445-475	62.81	0.75	16.41	7.44	0.13	2.36	1.34	0.98	3.00	0.12	4.66
	S15	5Bwcb	475-525	61.87	0.73	16.85	7.79	0.12	2.69	1.50	1.02	2.79	0.14	4.50
	S16	6Bcb	525-545	54.75	0.64	13.51	5.85	0.11	2.41	9.29	0.95	2.46	0.14	9.90

Strat. Set	Sample	Horizon	Depth cm	Ba	Co	Cr	Cu	Ga	Hf	La	Nb	Nd	Ni
				mg kg <sup>-1</sup>									
I	S1	Apb	50-75	398	21	121	81	16	10	65	11	30	64
	S2	ABcb	75-100	396	22	148	34	18	11	73	12	29	90
	S3	Bwcb	100-135	404	20	139	25	14	9	63	9	26	58
	S4	C1	135-170	373	14	230	23	10	9	56	6	15	37
	S5	C2	170-185	382	22	149	24	15	12	74	12	29	69
II	S6	2Bcb	185-201	439	22	156	37	23	10	81	14	35	83
	S7	2Bessb1	201-225	449	24	167	39	24	9	83	14	32	110
	S8	2Bessb2	225-271	440	25	176	44	26	10	81	17	35	123
	S9	2Bckb1	271-335	443	22	164	44	26	11	75	15	33	110
	S10	2Bckb2	335-365	435	22	167	47	27	9	83	19	33	118
III	S11	3Bcb	365-377	422	19	113	40	22	8	72	13	26	77
	S12	4Ab1	377-385	456	22	143	45	26	9	74	13	37	96
	S13	4Ab2	385-445	469	23	138	42	26	11	71	17	34	88
IV	S14	5Ab	445-475	465	20	132	34	20	14	76	15	28	73
	S15	5Bwcb	475-525	461	21	149	33	21	13	77	13	31	88
	S16	6Bcb	525-545	381	19	118	29	18	8	65	13	22	77

Strat. Set	Sample	Horizon	Depth cm	Pb	Rb	S	Sc	Sr	Th	V	Y	Zn	Zr
				mg kg <sup>-1</sup>									
I	S1	Apb	50-75	41	112	6	12	111	4	76	19	93	202
	S2	ABcb	75-100	21	119	5	15	93	6	96	22	82	173
	S3	Bwcb	100-135	20	105	6	13	92	3	68	18	84	170
	S4	C1	135-170	20	103	5	8	78	1	40	12	33	131
	S5	C2	170-185	24	110	6	12	109	3	71	27	56	262
II	S6	2Bcb	185-201	21	150	15	19	111	6	120	23	113	162
	S7	2Bessb1	201-225	21	154	24	20	114	6	132	24	113	145
	S8	2Bessb2	225-271	24	178	21	21	125	7	139	28	124	146
	S9	2Bckb1	271-335	20	155	26	18	126	6	136	23	120	130
	S10	2Bckb2	335-365	26	185	22	21	156	6	145	28	126	138
III	S11	3Bcb	365-377	22	120	32	19	170	5	117	20	97	123
	S12	4Ab1	377-385	19	155	27	18	129	6	134	20	124	119
	S13	4Ab2	385-445	22	181	19	21	131	8	130	27	116	185
IV	S14	5Ab	445-475	24	159	13	16	131	8	97	33	84	310
	S15	5Bwcb	475-525	23	122	19	15	119	7	96	28	81	260
	S16	6Bcb	525-545	21	95	25	17	158	5	90	28	69	243



Table 4

sample	Total carbon (analyzed at 950 °)		Organic carbon (analyzed at 450 °)	
	wt %	$\delta^{13}\text{C}$	wt %	$\delta^{13}\text{C}$
S1	0.92	-24.15	0.65	-24.73
S2	0.42	-24.22	0.31	-24.63
S3	0.27	-22.02	0.22	-24.45
S4	0.13	-22.70	0.13	-23.83
S5	0.17	-23.97	0.15	-24.58
S6	0.33	-24.66	0.26	-24.65
S7	0.55	-19.35	0.40	-24.76
S8	0.50	-21.53	0.37	-24.36
S9	0.76	-17.10	0.36	-24.13
S10	1.01	-16.96	0.46	-24.54
S11	1.72	-11.46	0.37	-24.78
S12	1.16	-18.78	0.57	-25.05
S13	1.01	-23.50	0.69	-25.01
S14	0.76	-23.65	0.58	-25.18
S15	0.46	-22.33	0.40	-24.41
S16	2.00	-12.99	0.36	-23.59